Supplementary Information

Convergent evolution enables eicosanoid precursor biosynthesis by ‘first’ fatty acyl desaturases in insects

Michal Tupec*, Ondřej Lukšan, Stanislav Macháček, Jan Křivánek, Iva Pichová, Robert Hanus*

Institute of Organic Chemistry and Biochemistry of the Czech Academy of Sciences, Prague, Czech Republic
*Corresponding authors, e-mails: tupec@uochb.cas.cz; robert.hanus@uochb.cas.cz

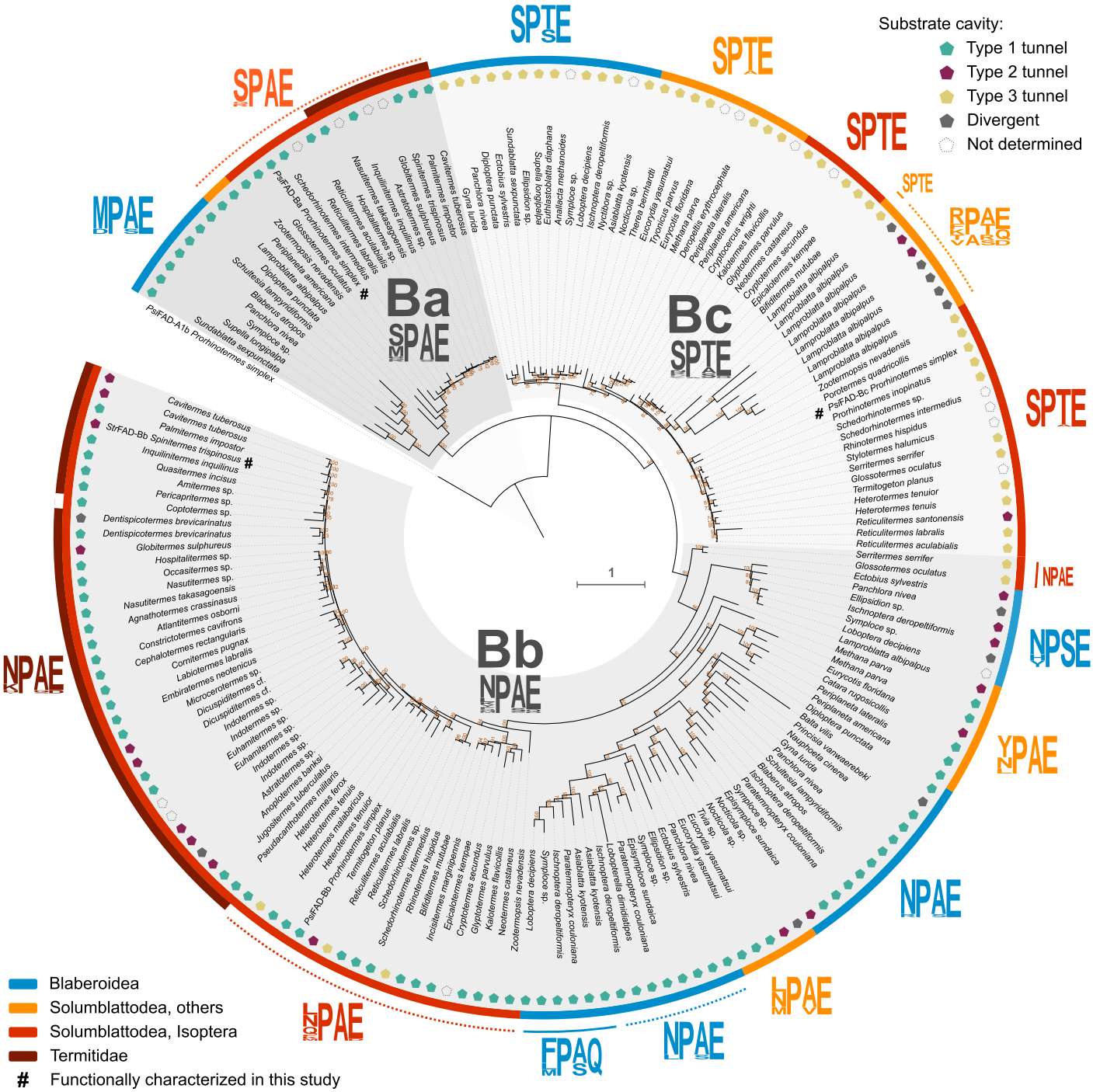

Supplementary Figure 1. Phylogeny and substrate cavity architecture of the FAD-Bs in Blattodea. A phylogenetic tree of blattodean desaturases from FAD-B subfamily, branching to Ba, Bb and Bc groups, including the observed substrate cavity architecture based on inspection of AlphaFold models. Δ9 FAD from *Prorhinotermes simplex*[1] was used as an outgroup protein. The signature motifs[2] of taxonomic FAD-B divisions are indicated as colored sequence logos. Accession numbers of all used protein sequences and summary data on the generated protein models are provided in Supplementary Data 1, and predicted models are provided in Supplementary Data 2.

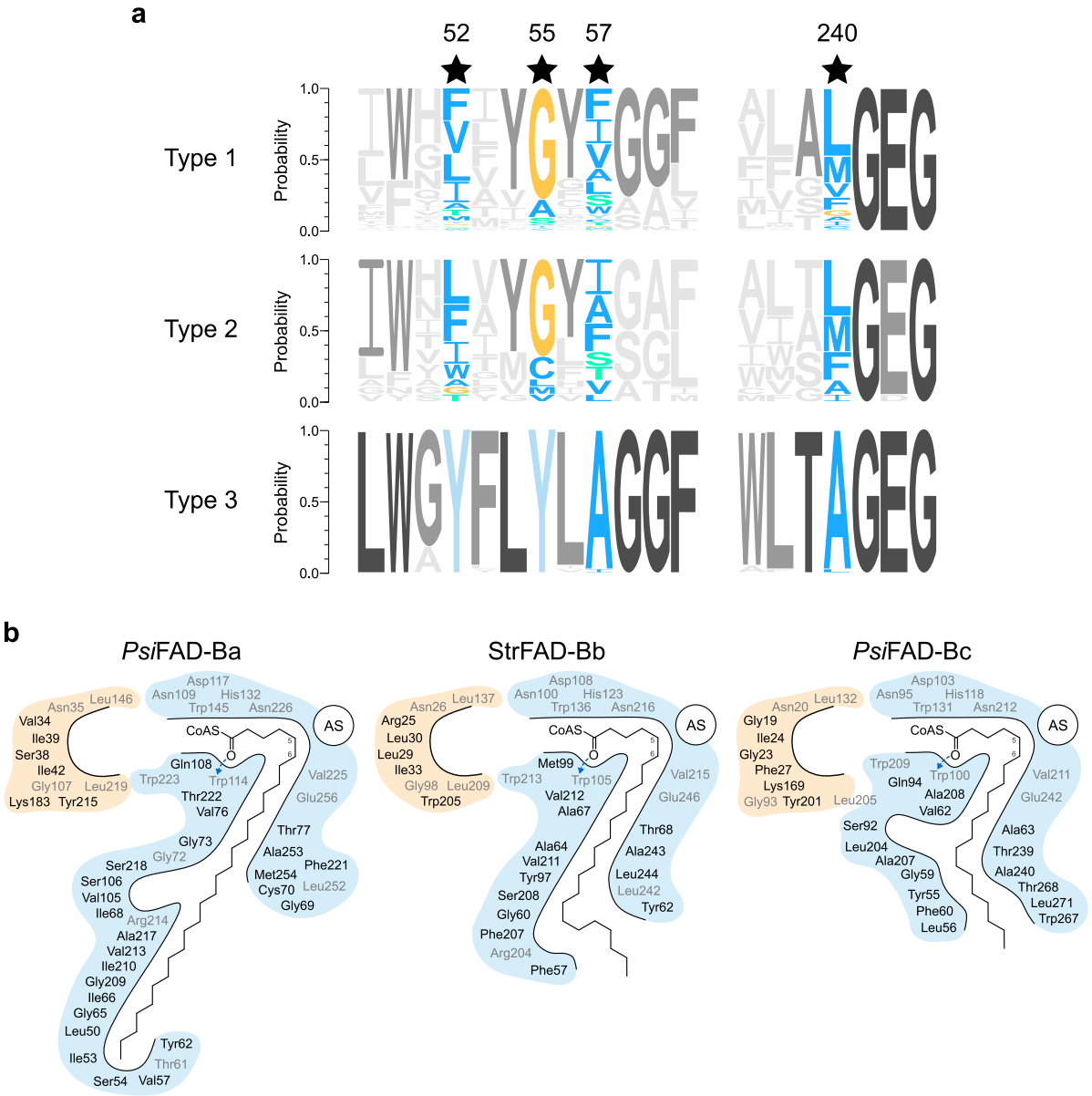

Supplementary Figure 2. Substrate tunnel conservation in blattodean FAD-Bs. a Sequence logos of the vicinity of residues (indicated by stars) which putatively determine where type 1, type 2 and type 3 substrate tunnel opens. Based on the alignment of blattodean FAD-Bs from Supplementary Fig. 1 (numbering based on the sequence of *Psi*FAD-Bc, a FAD-Bc from *P. simplex*). **b** Residue-level two-dimensional representations of termite FAD-B (*Psi*FAD-Ba, *Psi*FAD-Bc, with *Str*FAD-Bb, a FAD-Bb from *Spinitermes trispinosus*) external cavities (orange) and substrate tunnels (blue), as manually inferred from AlphaFold-generated models. Identical residues at structurally homologous positions are colored grey. The most favored saturated substrate (see Fig. 4b) is aligned into the tunnel of each enzyme, including the presumed positioning of C_1 acyl moiety with regard to the active site (AS) which is required for $\Delta 5$ regiospecificity. The putative hydrogen bonding of C_1 carbonyl to tryptophan residue (i.e., possible acyl register) is indicated by an arrow.

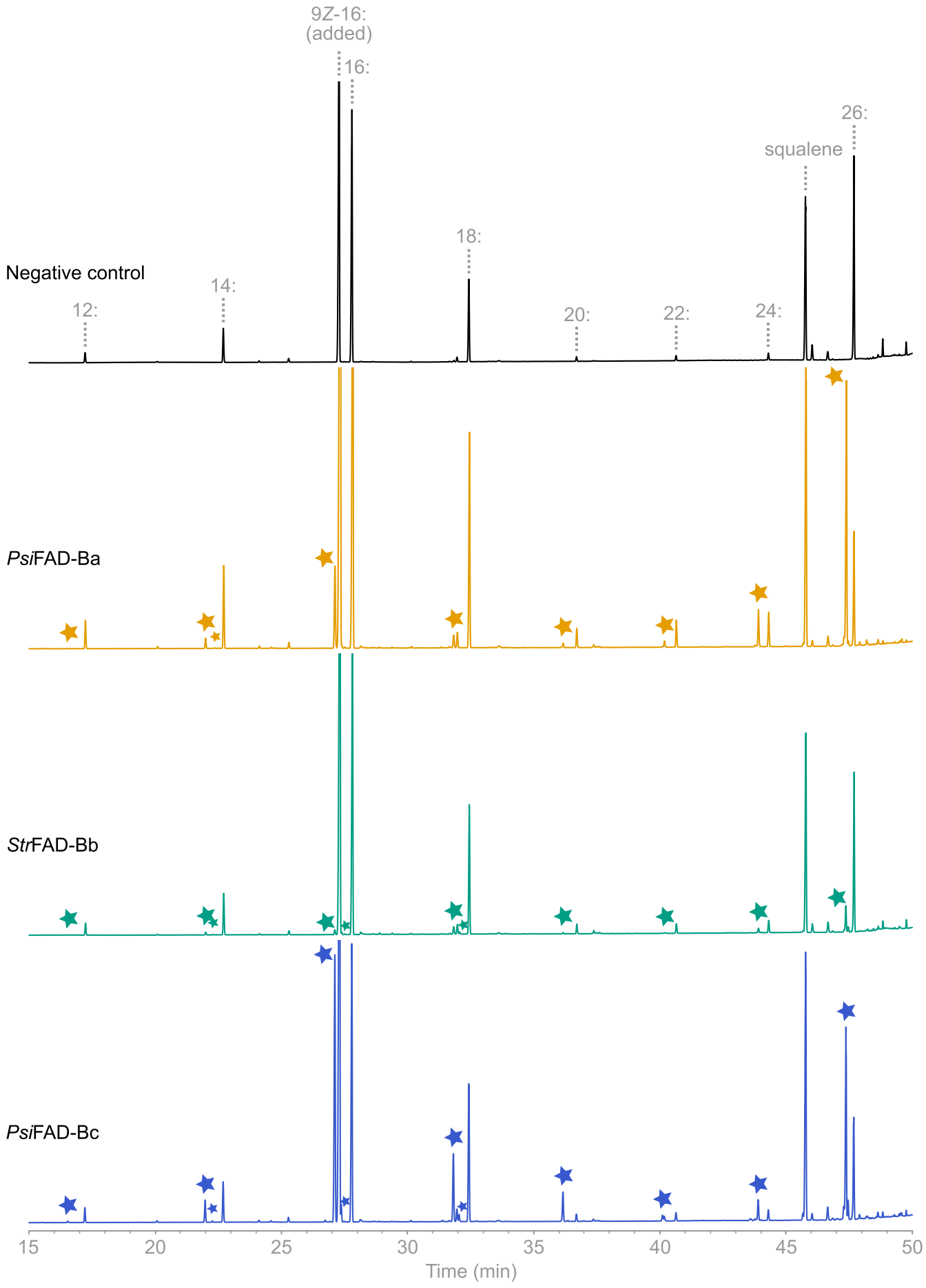

Supplementary Figure 3. Production of unsaturated FAs by termite FAD-Bs. Selected sections of chromatograms of FA methyl ester (FAME) extracts from yeast expressing *Psi*FAD-Ba, *Str*FAD-Bb and *Psi*FAD-Bc. Novel FAD-B-specific peaks are indicated by stars. The data were acquired using GC-FID.

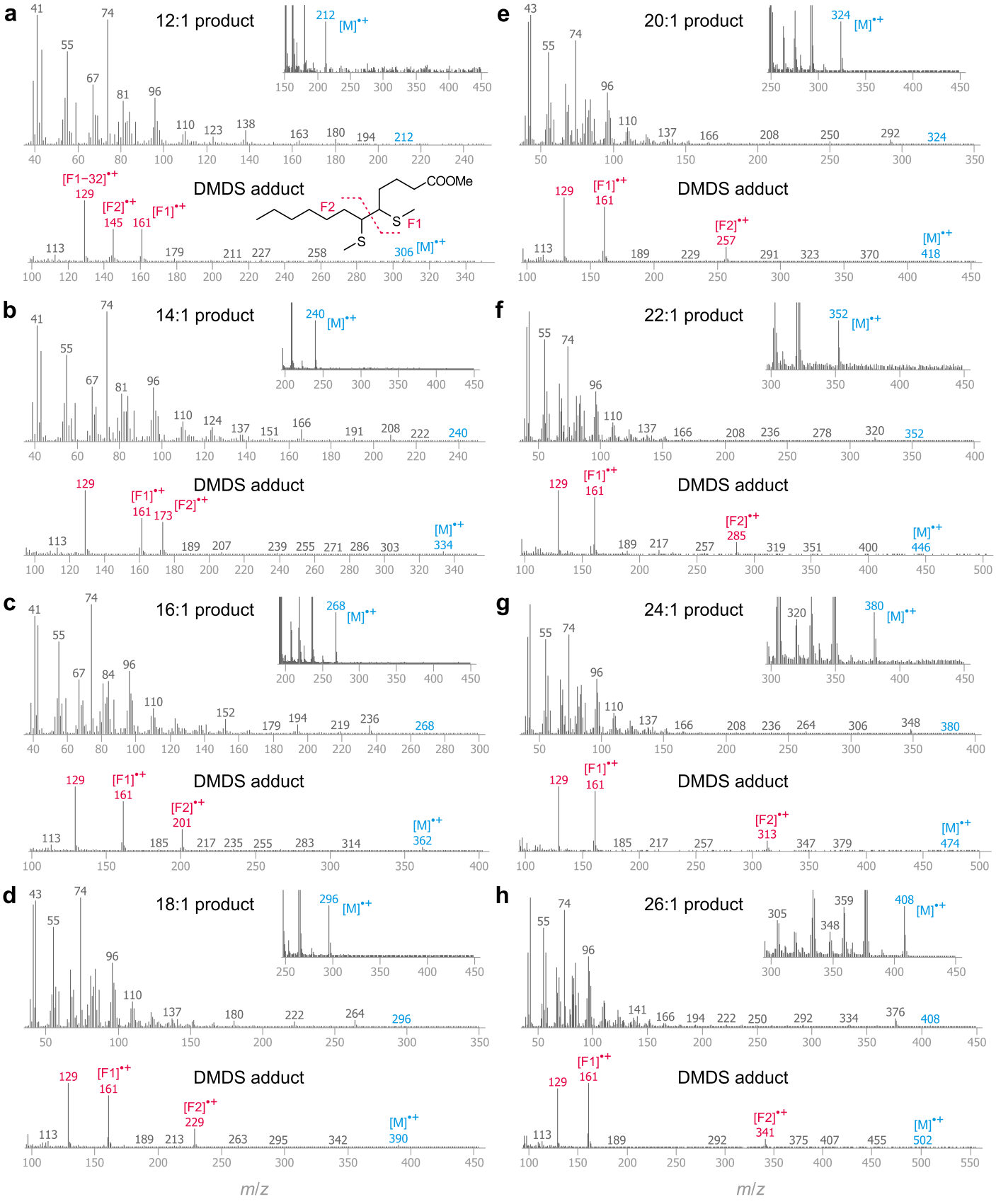

Supplementary Figure 4. Mass spectrometric characterization of major MUFA products. a–h Representative mass spectra of C12–C26 5*Z*-unsaturated FAs (*top*: FAME derivatives, *bottom*: sections of spectra of dimethyl disulfide (DMDS) adducts of the respective FAME derivatives) produced in yeast upon expression of FAD-B enzymes. The diagnostic ions arising from C_5–C_6 bond cleavage in DMDS adducts, as depicted in panel **a**, are denoted F1 (acyl part) and F2 (alkyl part). The data were acquired using GC×GC-MS.

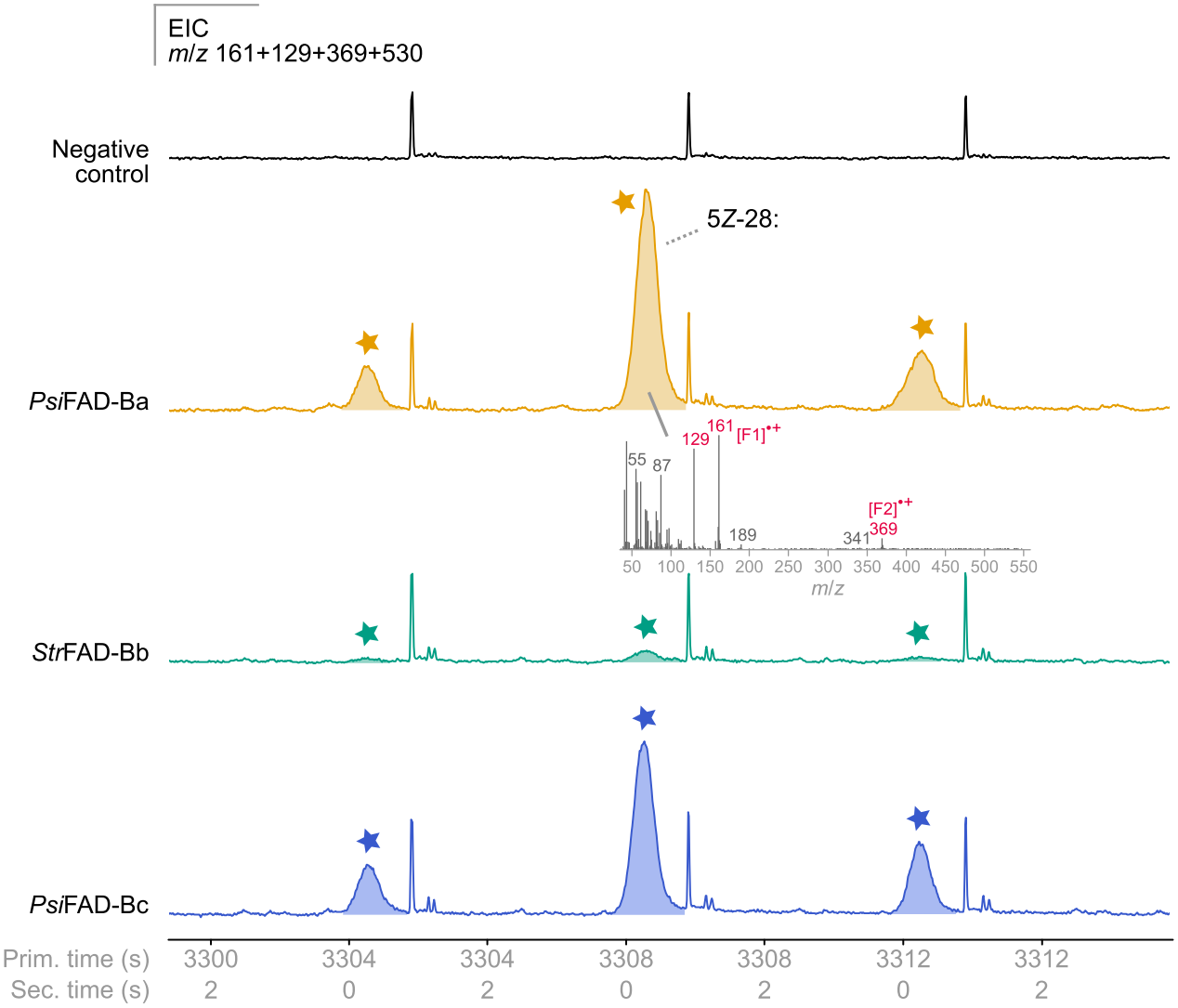

Supplementary Figure 5. Production of unsaturated C28 FA by termite FAD-Bs. Selected sections of chromatograms of DMDS-derivatized FAME extracts from yeast upon expression of termite FAD-Bs. The peaks of FAD-B-specific product are highlighted with stars. The data were acquired using GC×GC-MS.

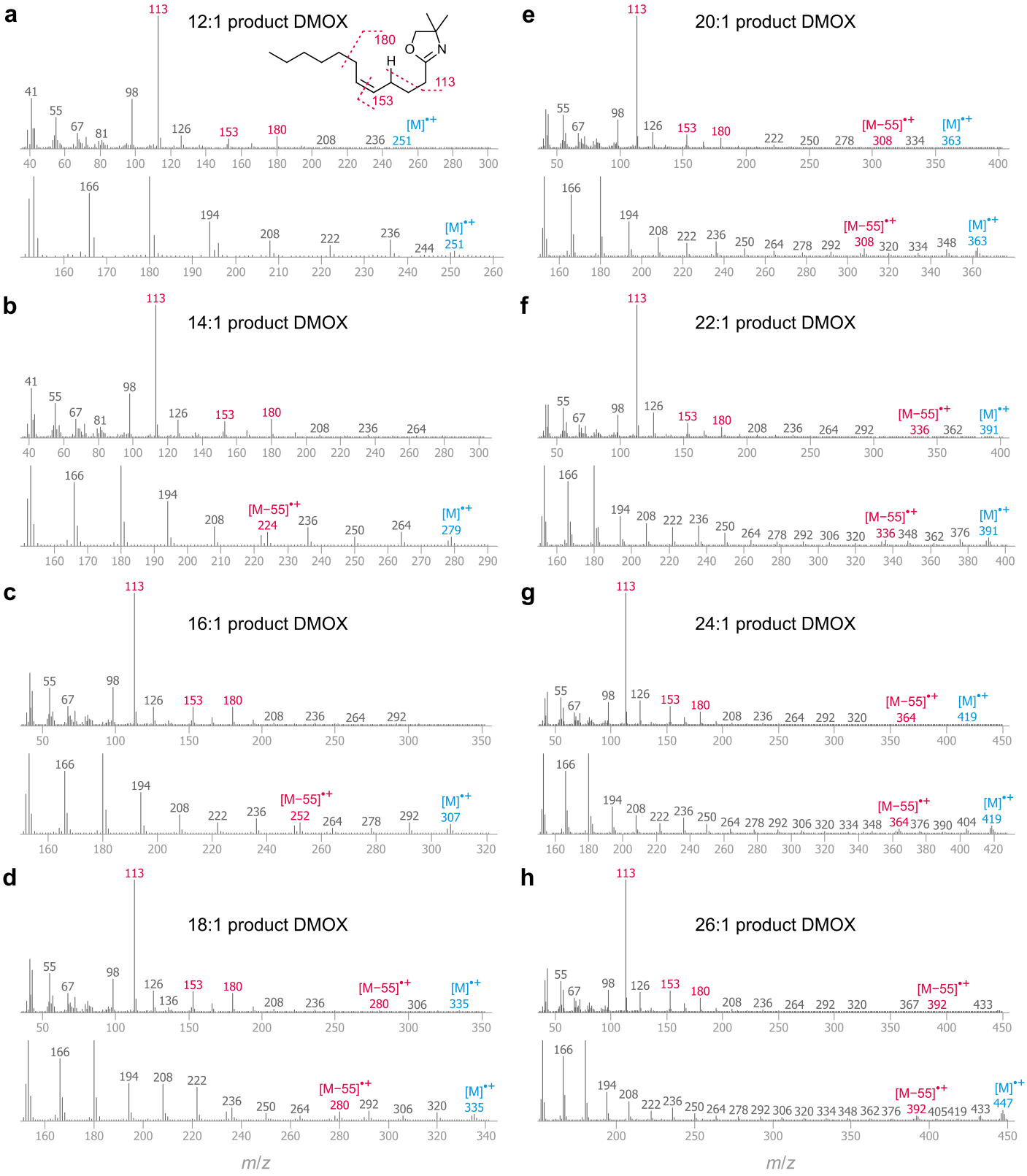

Supplementary Figure 6. Mass spectrometric characterization of DMOX derivatives of major MUFA products. a–h Representative mass spectra of C12–C26 5*Z*-unsaturated FAs, which are produced in yeast upon expression of FAD-B enzymes, converted into DMOX derivatives (*top*: spectra, *bottom*: spectra zoomed at lower-abundance *m*/*z* region). The diagnostic ions including those which form as depicted in panel **a** (e.g., McLafferty ion) are highlighted. The data were acquired using GC×GC-MS.

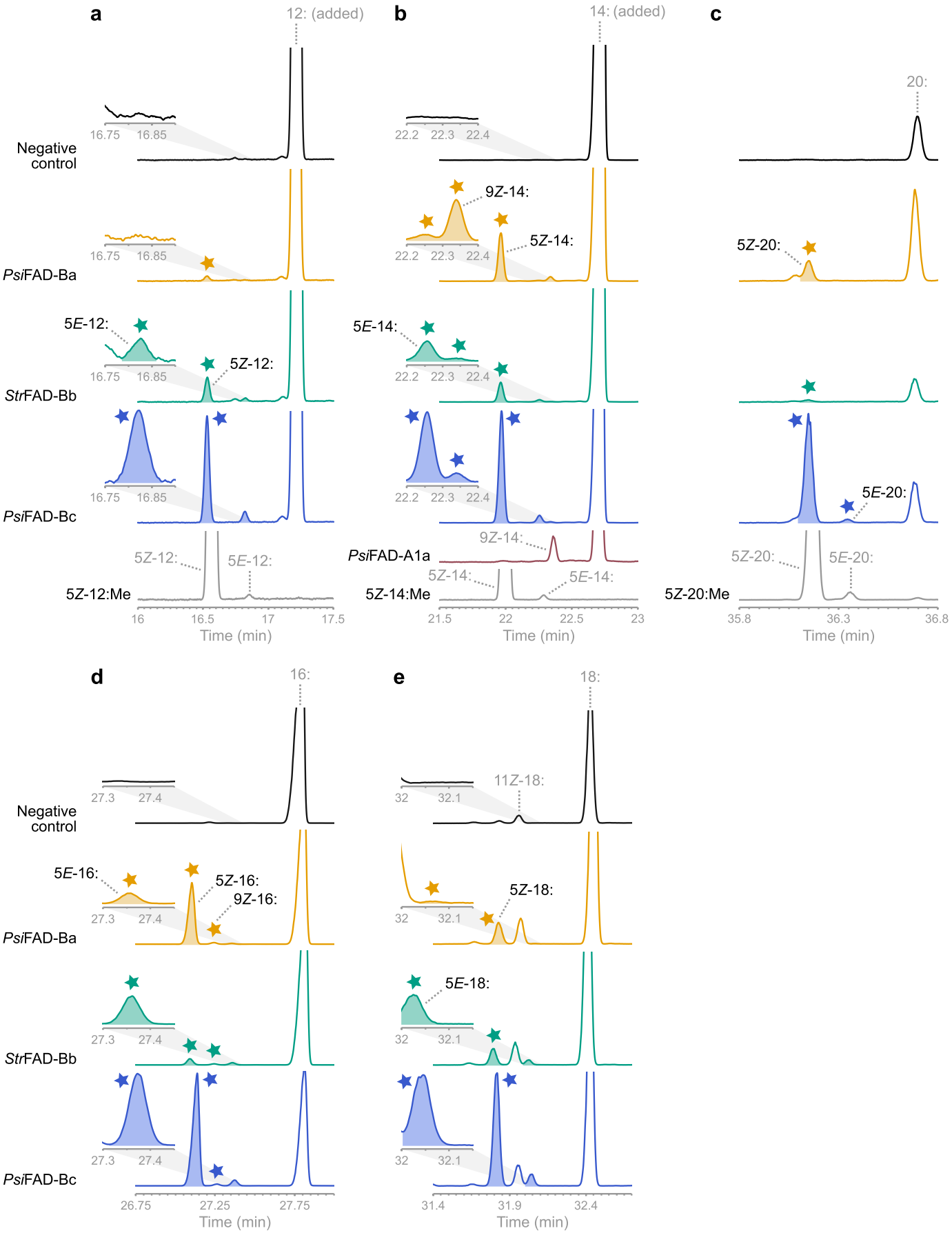

Supplementary Figure 7. Production of unsaturated C12 to 20 FAs by termite FAD-Bs. a–e Sections of chromatograms of FAME extracts from yeast supplemented with 12:Me (**a**), 14:Me (**b**), 17:Me (**c**), oleic acid (OA, **d**), and palmitoleic acid (POA, **e**) upon expression of termite FAD-Bs and of 5*Z*-12:Me, 5*Z*-14:Me, and 5*Z*-20:Me standards. GC trace of FAME extract from yeast expressing *Psi*FAD-A1a[1], a reference for 9*Z*-14: product, is included in **b**. The peaks of FAD-B-specific products are indicated by stars. The data were acquired using GC-FID.

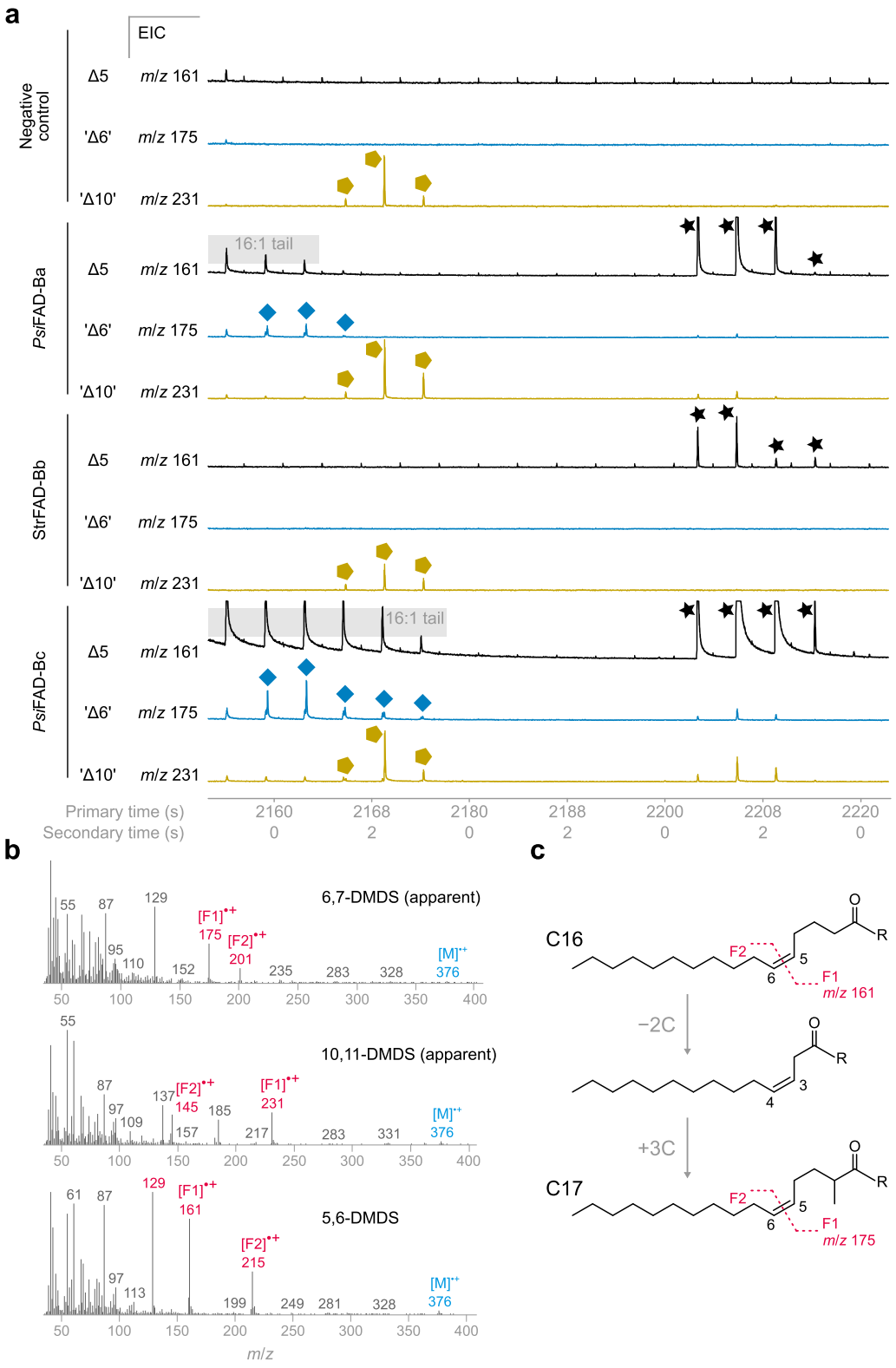

Supplementary Figure 8. Formation of unsaturated odd-chain FAs in yeast. a Partial extracted ion chromatograms (EICs) of DMDS-derivatized FAME extracts from yeast expressing termite FAD-Bs supplemented with 17:. The 5,6-DMDS adducts, and apparent 6,7-DMDS and 10,11-DMDS adducts are selectively visualized using *m*/*z* of 161, 175 and 231, respectively. The 5-unsaturated FAs produced by FAD-B enzymes are indicated by stars. The likely methyl-branched 5- and 9-unsaturated FAs, which putatively form from 5*Z*-16: and 9*Z*-16: via a yeast metabolic process, are denoted with rectangles and pentagons, respectively. The data were acquired using GC×GC-MS. **b** Representative mass spectra of DMDS adducts of monounsaturated C17 FAs extracted from yeast expressing FAD-B enzymes supplemented with 17:. The diagnostic ions are highlighted analogously to those in Supplementary Fig. 4. The presented spectra originate from Bc sample. The data were acquired using GC×GC-MS. **c** Proposed formation of branched odd-chain unsaturated FAs by β-oxidation–elongation process in yeast. The *m*/*z* of $[F1]^{\bullet+}$ fragment ion arising from the respective DMDS adduct is indicated.

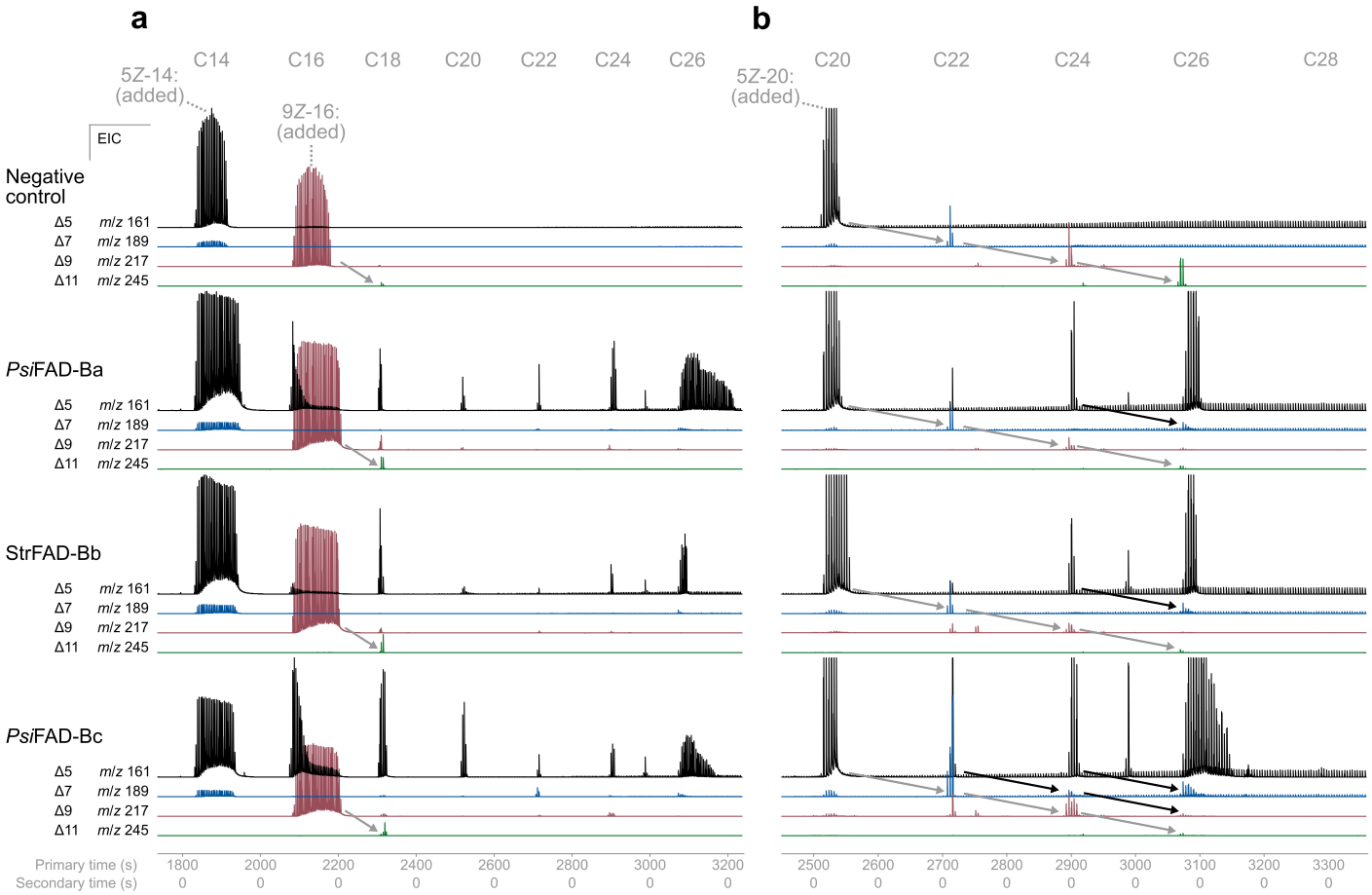

Supplementary Figure 9. Elucidation of FA elongation patterns in yeast. ab Partial extracted ion chromatograms of DMDS-derivatized extracts from yeast expressing FAD-B enzymes supplemented with 5*Z*-14: (**a**) or 5*Z*-20: (**b**). The 5,6-DMDS, 7,8-DMDS, 9,10-DMDS and 11,12-DMDS adducts are selectively visualized using *m*/*z* of 161, 189, 217 and 245, respectively. The FA elongations which derive from the added FA(s) are indicated by grey arrows. Black arrows represent FA elongations which depend on FAD-specific products. The small peaks of 9*Z*-18: are likely a remnant of growing the yeast starter colonies on solid medium with both POA and OA. The data were acquired using GC×GC-MS.

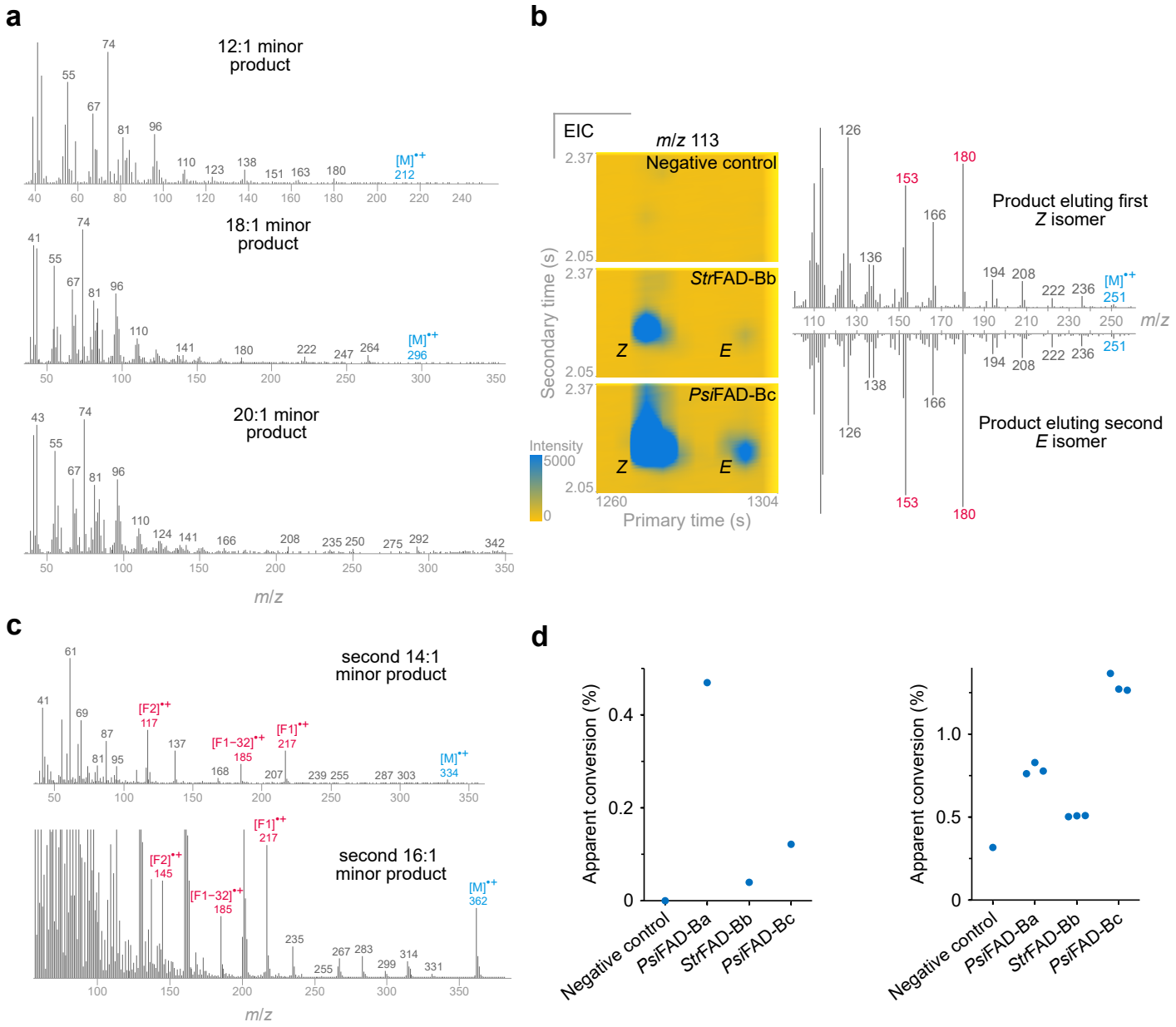

Supplementary Figure 10. Mass spectrometric characterization of minor MUFA products. **a** Representative mass spectra of minor C12, C18 and C20 5-unsaturated FAs produced in yeast supplemented with 12:Me (*top* spectrum) or just POA (two *bottom* spectra) upon expression of FAD-B enzymes. The shown spectra originate from the Bc sample. **b** *left* Contour plot sections of extracted ion chromatograms (at *m*/*z* 113) of 2-amino-2-methyl-1-propanol (AMP)-derivatized extracts from yeast expressing Bb and Bc enzyme. *right* Selected sections of mass spectra of 5*Z*-12:DMOX (*top*) and 5*E*-12:DMOX (*bottom*) product peaks from the Bc sample. The diagnostic ions are highlighted. **c** Representative mass spectra of DMDS-derivatized C14, and C16 9-unsaturated FAs produced in yeast upon expression of FAD-B enzymes. The diagnostic ions are highlighted. The spectrum of 9*Z*-16: predominantly contains fragments of the coeluting 5*Z*-16: product. The shown spectra originate from Ba (*top*) and Bc (*bottom*) samples. The data in **a**–**c** panels were acquired using GC×GC-MS. **d** Apparent conversions of 14: and 16: substrates into corresponding 9-unsaturated products in yeast expressing termite FAD-Bs supplemented with 14: (*left*) and OA (*right*). Determined by GC-FID analysis of FAME extracts (n = 1, n = 3). Basal level of 9*Z*-16: detected in the negative control presumably derives from yeast colonies, grown on both POA and OA, that were used for inoculation.

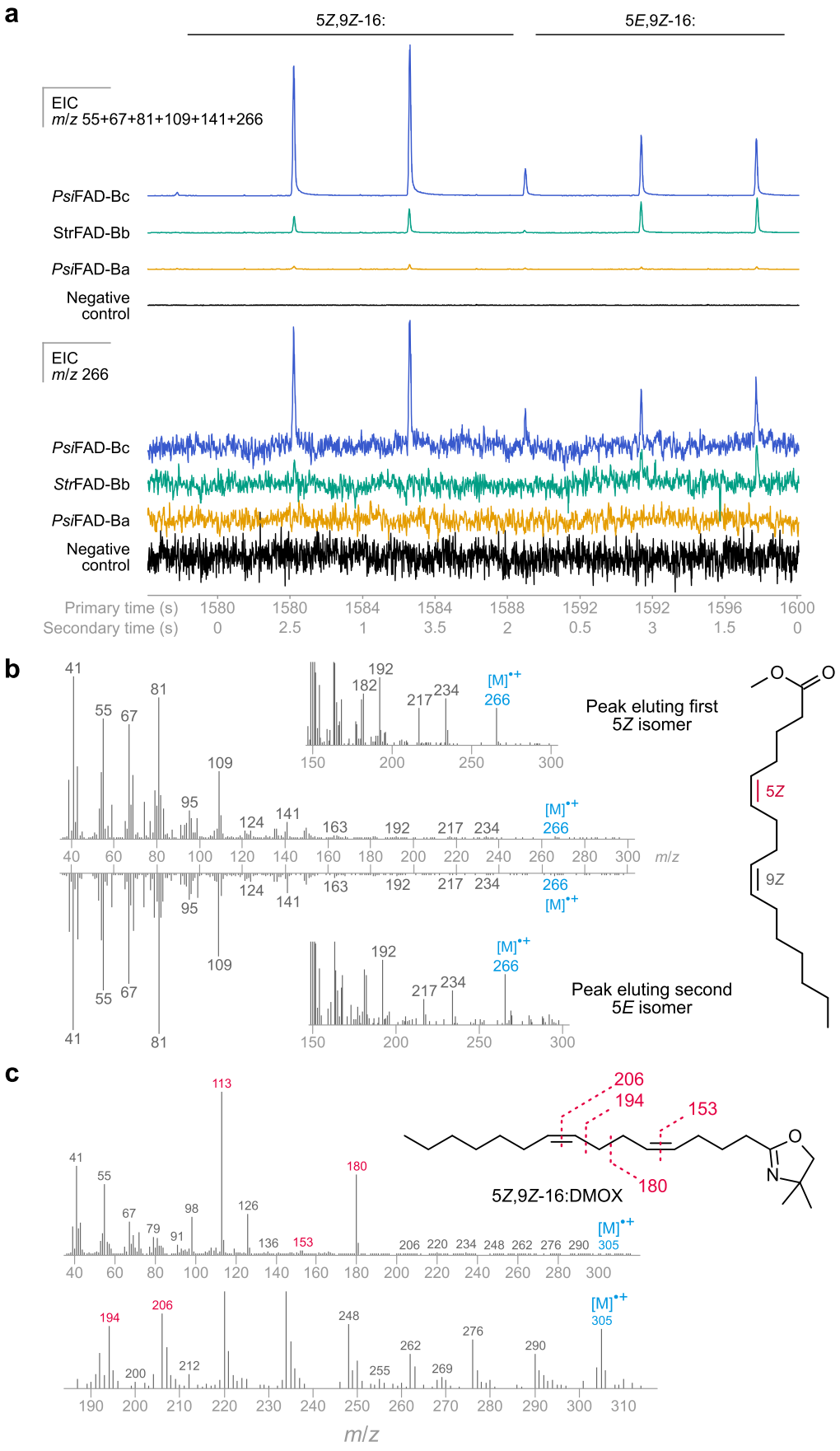

Supplementary Figure 11. Production of C16 dienoic FAs by termite FAD-Bs. **a** Selected sections of extracted ion chromatograms of FAME extracts from yeast supplemented with POA expressing termite FAD-Bs, illustrating production of two dienoic C16 isomers. **b** Representative mass spectra of isomeric 5,9-diunsaturated C16s with the structure of 5*Z*,9*Z*-16:Me shown. **c** Representative mass spectrum of 5*Z*,9*Z*-16: product converted into DMOX derivative (*top*: spectrum, *bottom*: spectrum zoomed at lower-abundance *m*/*z* region). The diagnostic ions are highlighted. The shown spectra originate from Bc sample. The data were acquired using GC×GC-MS.

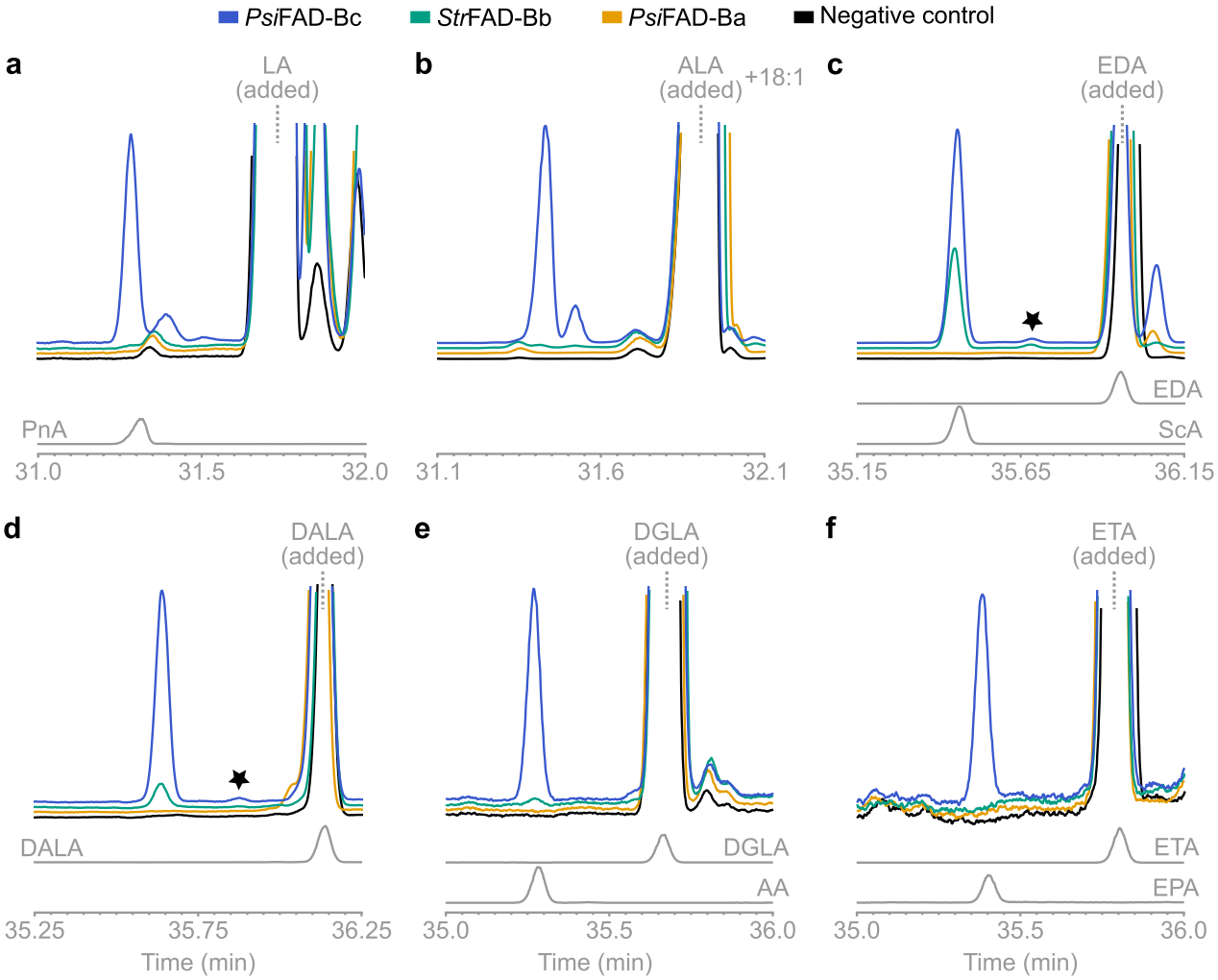

Supplementary Figure 12. Production of PUFAs by termite FAD-Bs. a–f Sections of chromatograms of FAME extracts from yeast expressing termite FAD-Bs, supplemented with linoleic acid (**a**, LA), α-linolenic acid (**b**, ALA), 11*Z*,14*Z*-eicosadienoic acid (**c**, EDA), dihomo-α-inolenic acid (**d**, DALA), dihomo-γ-linolenic acid (**e**, DGLA) or 8*Z*,11*Z*,14*Z*,17*Z*-eicosatetraenoic acid (**f**, ETA), and of selected FAME standards: methyl pinolenate (PnA), EDA, methyl sciadonate (ScA), DALA, DGLA, methyl arachidonate (AA), ETA, methyl 5*Z*,8*Z*,11*Z*,14*Z*,17*Z*-eicosapentaenoate (EPA). The presumed 5*E*-unsaturated product isomers are indicated by stars. The data were acquired using GC-FID.

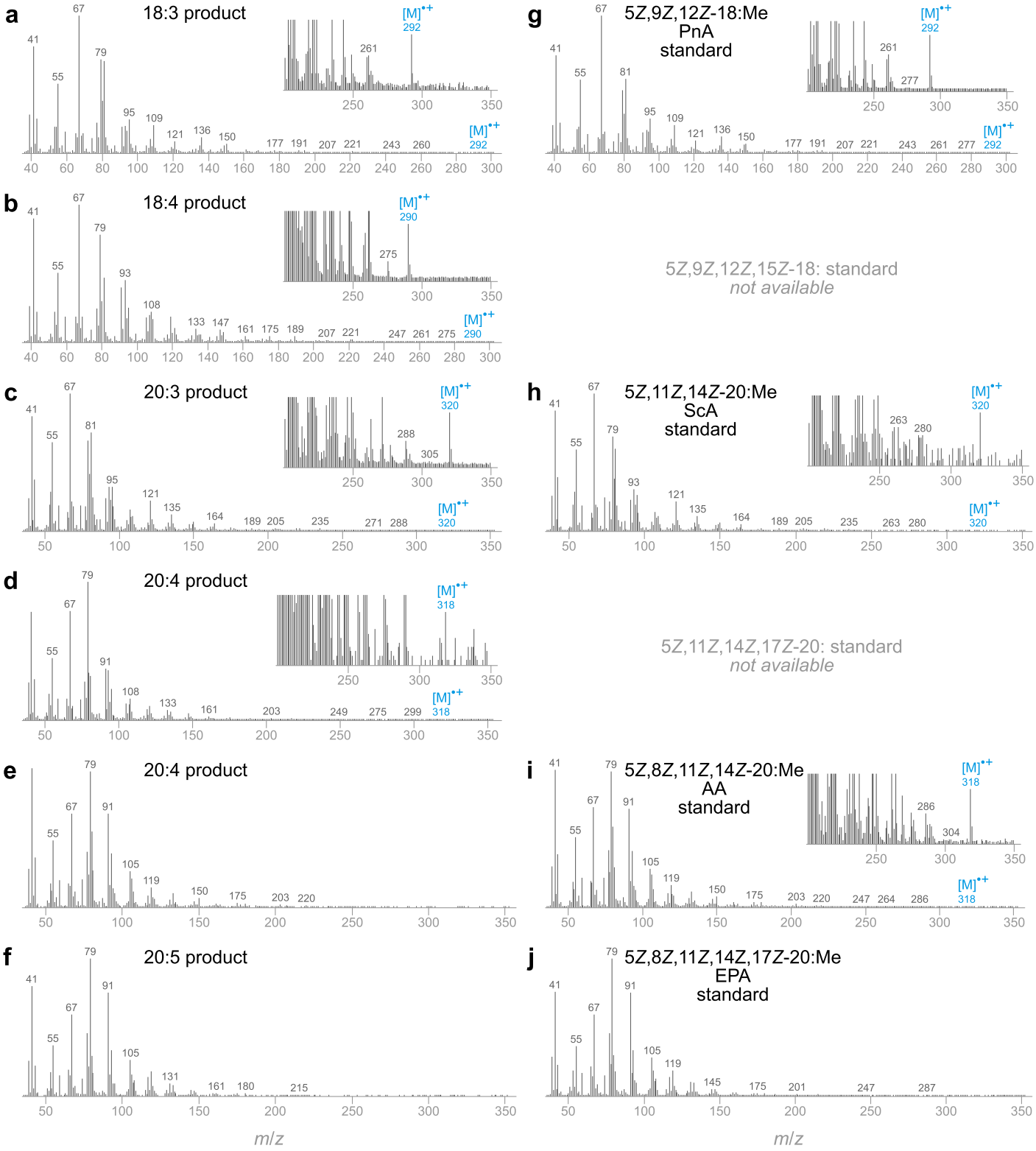

Supplementary Figure 13. Mass spectrometric characterization of PUFA products. a–f Representative mass spectra of 5*Z*-unsaturated PUFAs (FAME derivatives) produced in yeast supplemented with LA (**a**), ALA (**b**), EDA (**c**), DALA (**d**), DGLA (**e**), and ETA (**f**) upon expression of Bb or Bc enzyme. The shown spectra originate from Bc sample. **g–j** Mass spectra of PUFA standards: PnA (**g**), ScA (**h**), AA (**i**), EPA (**j**). The data were acquired using GC×GC-MS.

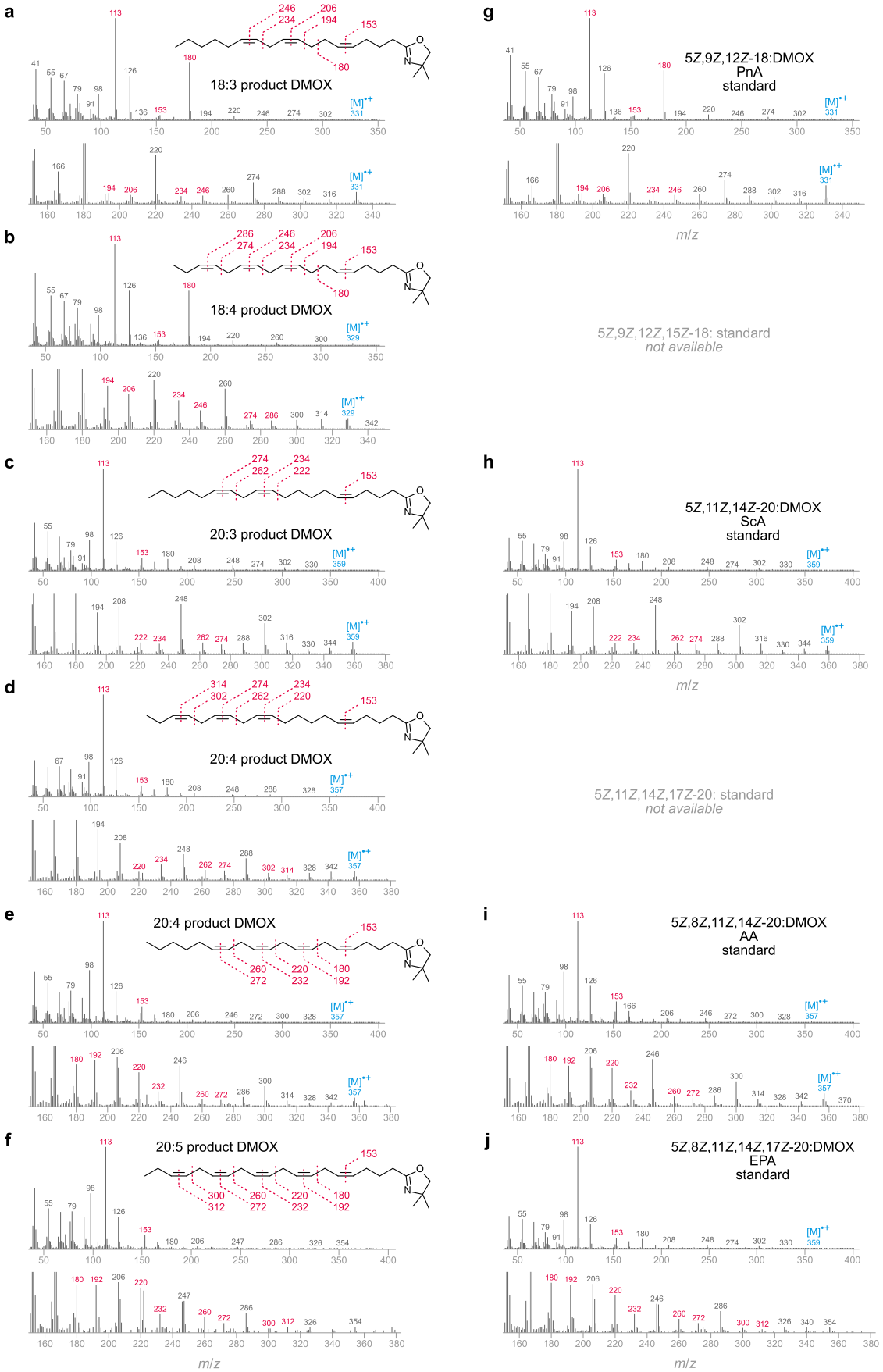

Supplementary Figure 14. Mass spectrometric characterization of DMOX derivatives of PUFA products. a–j Representative mass spectra of 5*Z*-unsaturated PUFAs (DMOX derivatives) produced in yeast supplemented with PUFA precursors (**a**, LA, **b**, ALA, **c**, EDA, **d**, DALA, **e**, DGLA, **f**, ETA) upon expression of Bb or Bc enzyme. The shown spectra originate from Bc sample. The fragmentations leading to diagnostic ions are indicated on individual FA structures. **g–j** Mass spectra of PUFA standards: PnA (**g**), ScA (**h**), AA (**i**), EPA (**j**). The data were acquired using GC×GC-MS.

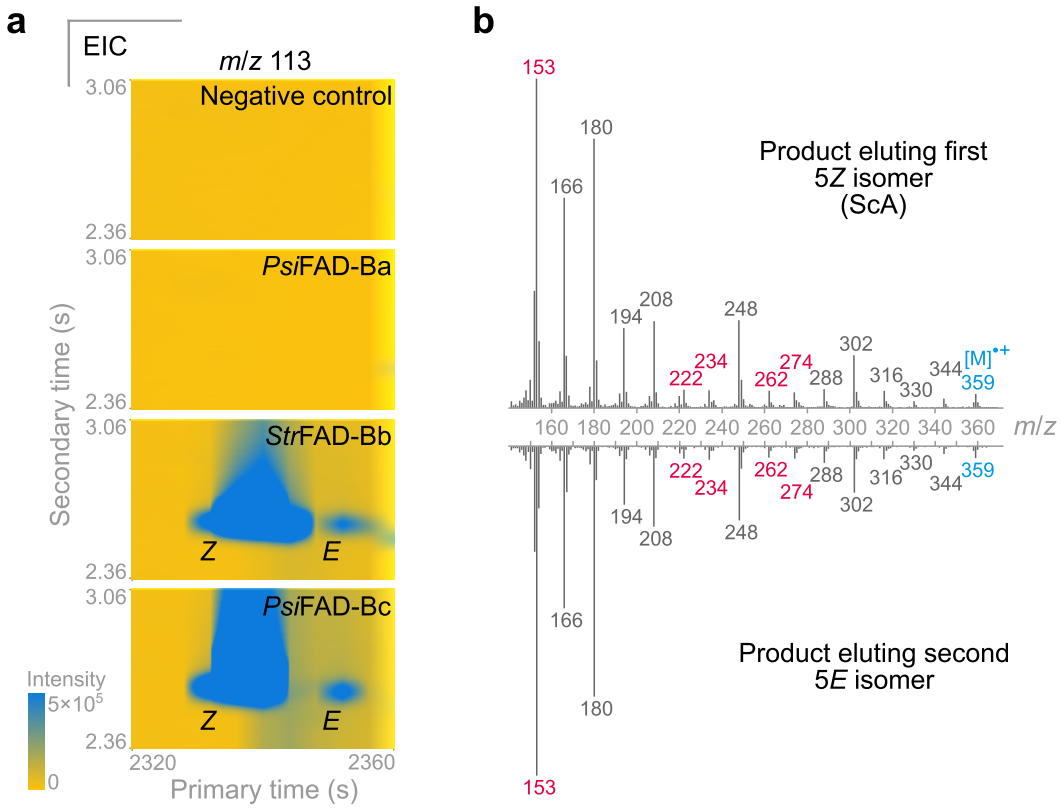

Supplementary Figure 15. Mass spectrometric characterization of 20:3 product isomers. a Contour plot sections of extracted ion chromatograms (at *m*/*z* 113) of AMP-derivatized extracts from yeast expressing FAD-B enzymes supplemented with EDA. **b** Selected sections of mass spectra of 5*Z*,11*Z*,14*Z*-20:DMOX (ScA; *top*) and 5*E*,11*Z*,14*Z*-20:DMOX (*bottom*) product peaks from the Bc sample. The diagnostic ions are highlighted. The data were acquired using GC×GC-MS.

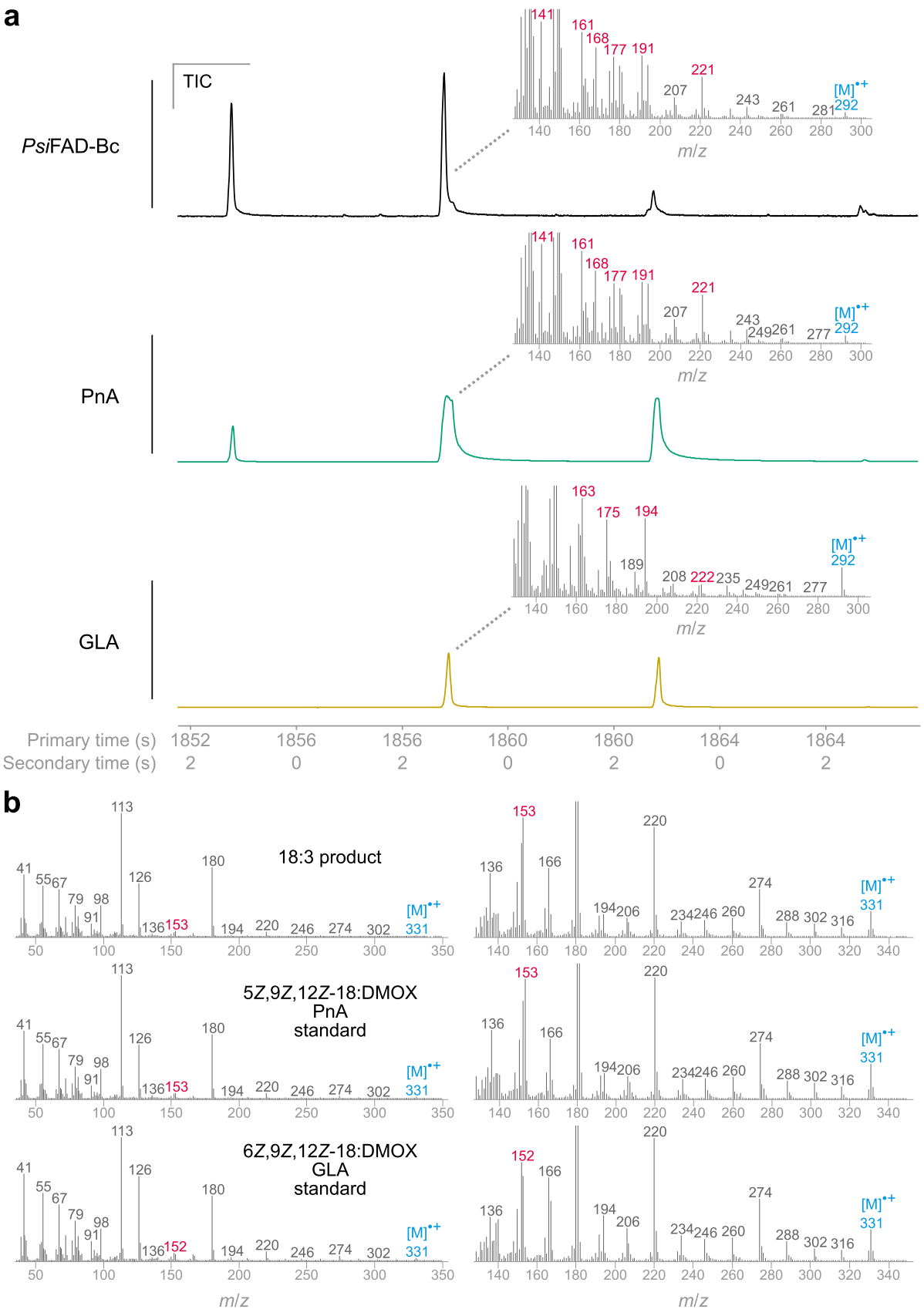

Supplementary Figure 16. Characterization of 18:3 product. a Sections of total ion chromatograms (TICs) of FAME extract from yeast expressing *Psi*FAD-Bc supplemented with LA and of FAME standards of pinolenic acid (PnA) and γ-linolenic acid (GLA), including partial mass spectra of selected peaks focused on distinct *m*/*z* region. The spectral features differing between PnA and GLA are highlighted. **b** Representative mass spectra of DMOX derivatives of 18:3 PUFAs produced in yeast supplemented with LA upon expression of Bb or Bc enzyme, and mass spectra of standards of PnA and GLA (*left*: spectra, *right*: spectra zoomed at lower-abundance *m*/*z* region). The *m*/*z* of 153 and 152 which reach different intensities in PnA and GLA spectra are highlighted. The top shown spectrum originates from Bc sample. The data were acquired using GC×GC-MS.

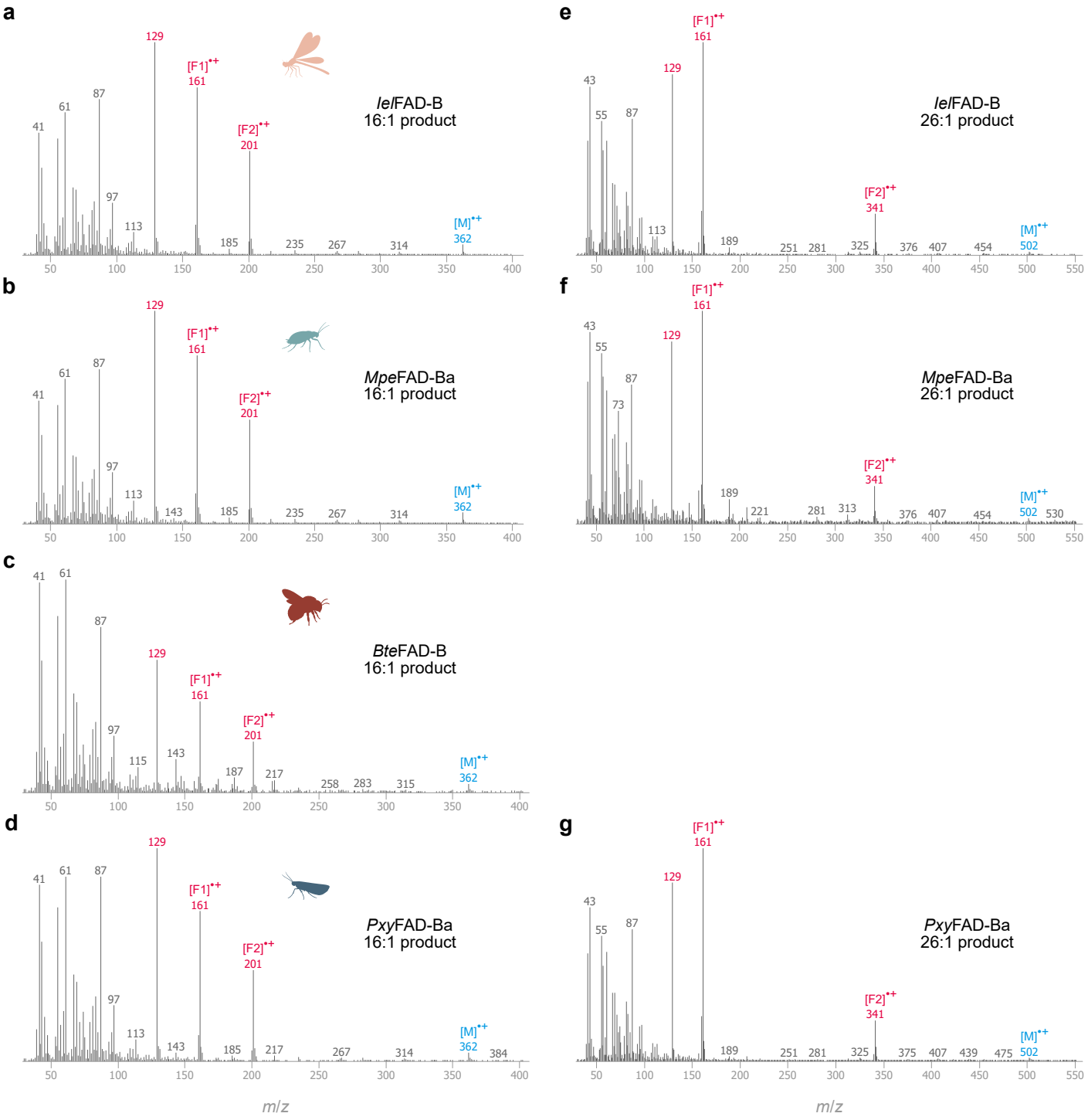

Supplementary Figure 17. Mass spectrometric characterization of MUFA products of insect FAD-Bs. **a**–**g** Representative mass spectra of DMDS adducts of the 5-unsaturated C16 (**a**–**d**) and C26 (**e**–**g**) FAs produced in yeast upon expression of FAD-Bs from *Ischnura elegans*, *Myzus persicae*, *Bombus terrestris*, and *Plutella xylostella*. The diagnostic ions arising from C_5–C_6 bond cleavage are highlighted. The data were acquired using GC×GC-MS.

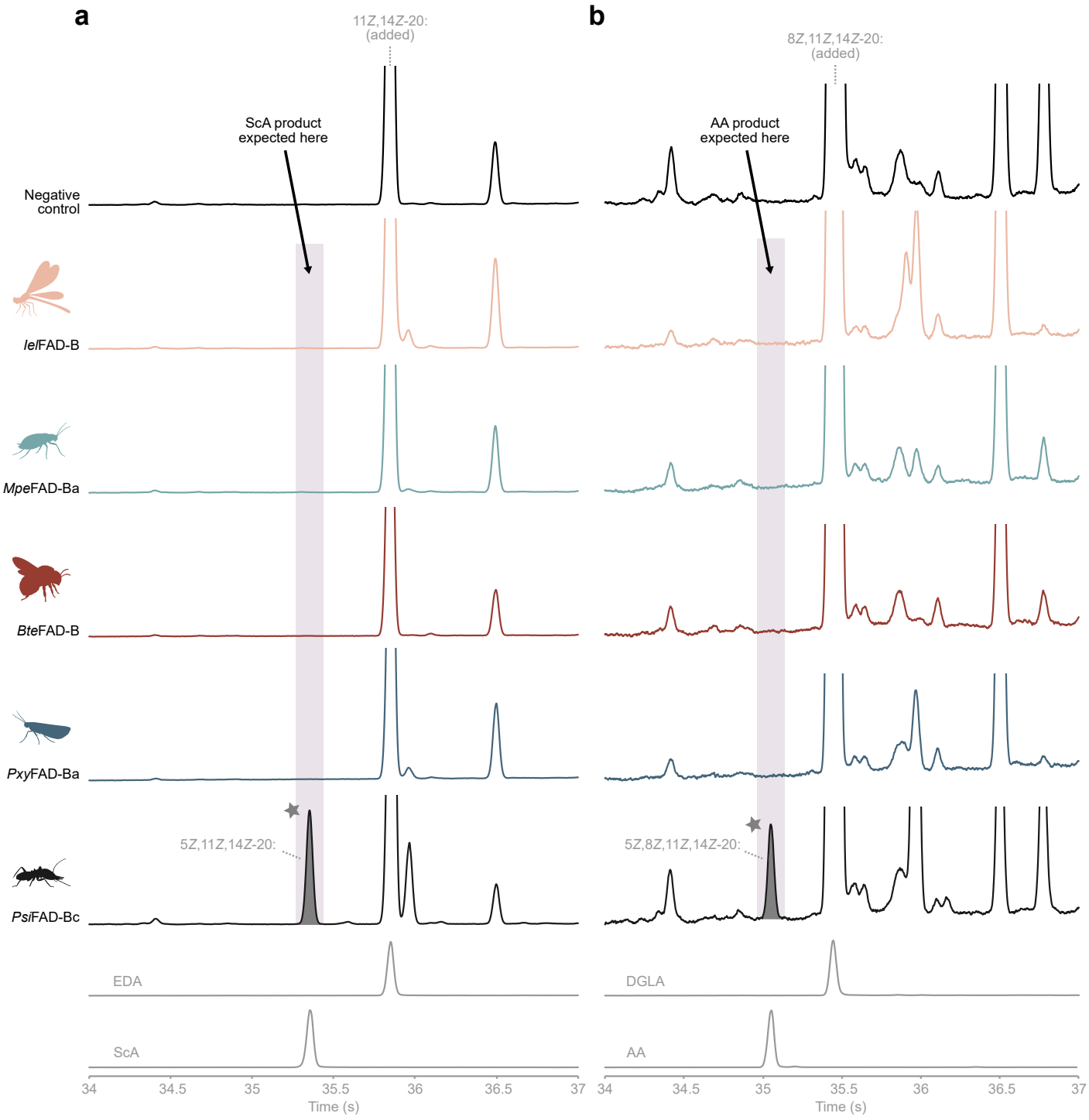

Supplementary Figure 18. Screening for Δ5 conversion of eicosadienoic and dihomo-γ-linolenic acid by insect FADs. ab Selected sections of chromatograms of FAME extracts from yeast expressing insect FADBs from *I. elegans*, *M. persicae*, *B. terrestris*, and *P. xylostella* (with *Psi*FAD-Bc used as a positive control), supplemented with EDA (**a**) or ScA (**b**), and of FAME standards. The data were acquired using GC-FID.

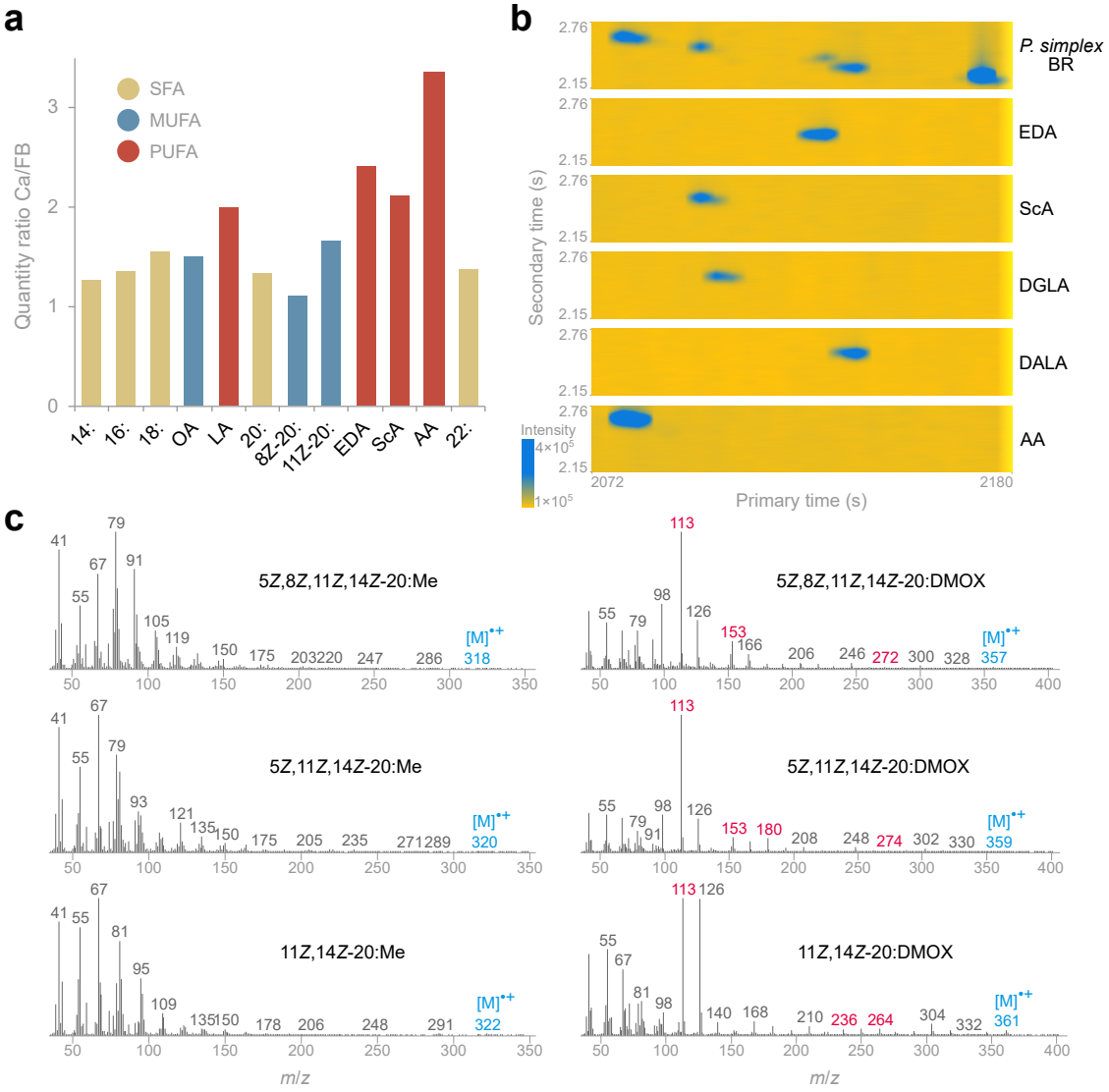

Supplementary Figure 19. FA pool in *Prorhinotermes simplex* **workers. a** Tissue-specific enrichment of certain FAs in *P. simplex* workers. Ratios of various fatty acyl quantities between carcass (Ca) and fat body (FB) tissue as determined by GC-FID. The saturated (SFAs), monounsaturated (MUFAs) and polyunsaturated FAs (PUFAs) are distinguished by colors. The FAME extracts of pooled tissues from ten *P. simplex* workers were used for quantification. Source data are available in Supplementary Data 1. **b** Contour plot sections of total ion chromatograms of FAME extract from *P. simplex* worker BR and of FAME standards of 11*Z*,14*Z*-eicosadienoic acid (EDA), sciadonic acid (ScA), dihomo-γ-linolenic acid (DGLA), dihomo-α-linolenic acid (DALA) and arachidonic acid (AA). The data were acquired using GC×GC-MS. **c** Mass spectra of major polyunsaturated C20 FAs detected in *P. simplex* workers BR total lipid extracts as FAMEs (*left*) and upon conversion to DMOX derivatives (*right*). The diagnostic ions are highlighted. The data were acquired using GC×GC-MS.

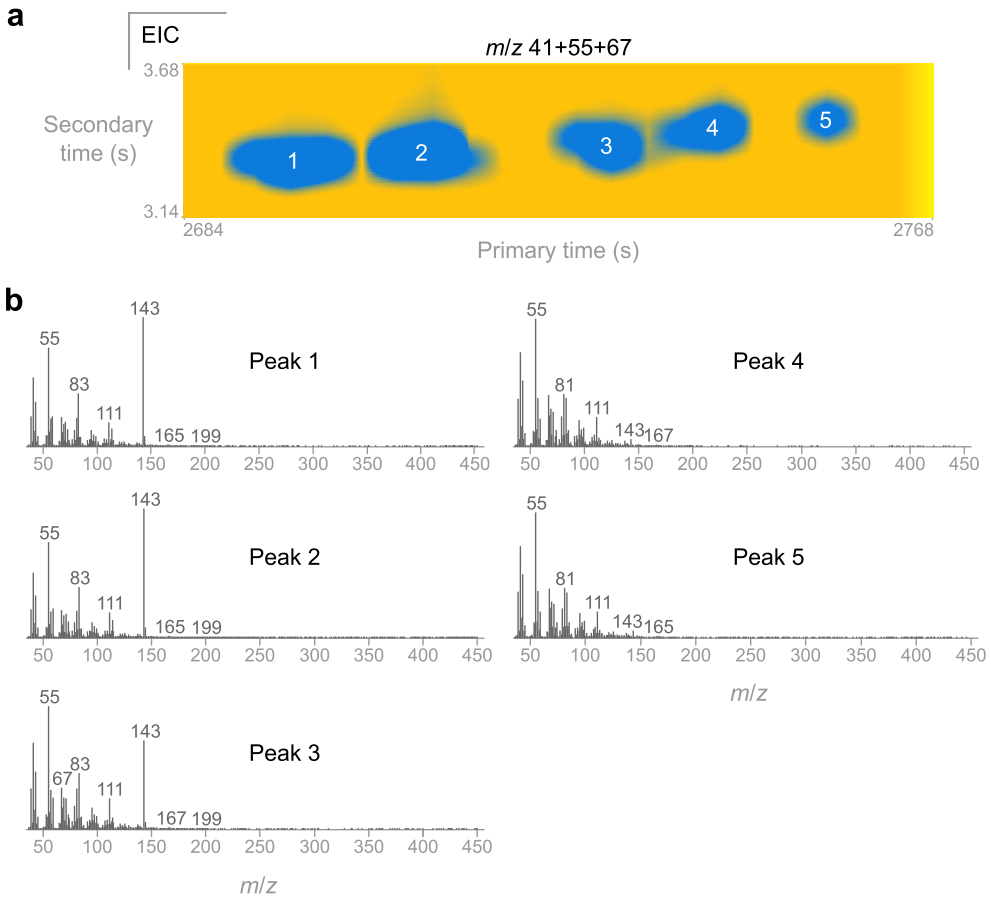

Supplementary Figure 20. MS characterization of epoxidized arachidonic acid fingerprint. a A contour plot section of extracted ion chromatogram (at *m/z* 41+55+67) of AA-derived products upon derivatization with *meta*-chloroperoxybenzoic acid (mCPBA). **b** Mass spectra of the respective peaks. The data were acquired using GC×GC-MS.

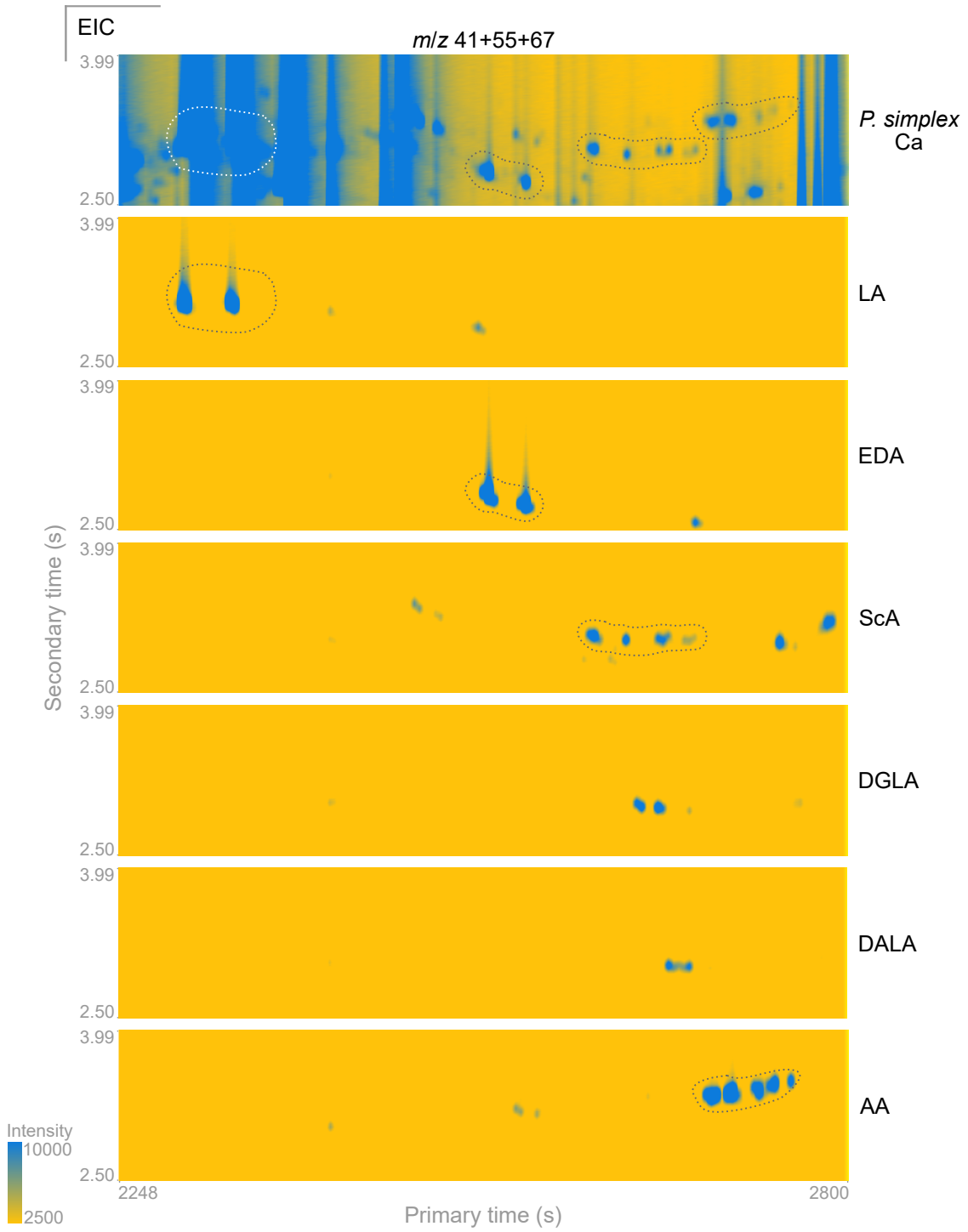

Supplementary Figure 21. Fingerprinting of major PUFAs from *P. simplex* workers upon epoxidation. Contour plot sections of extracted ion chromatograms (at *m*/*z* 41+55+67) of mCPBA-derivatized FAME extract from pooled carcasses (Ca) of ten *P. simplex* workers and FAME standards of linoleic acid (LA), 11*Z*,14*Z*-eicosadienoic acid (EDA), sciadonic acid (ScA), dihomo-γ-linolenic acid (DGLA), dihomo-α-linolenic acid (DALA) and arachidonic acid (AA). The data were acquired using GC×GC-MS.

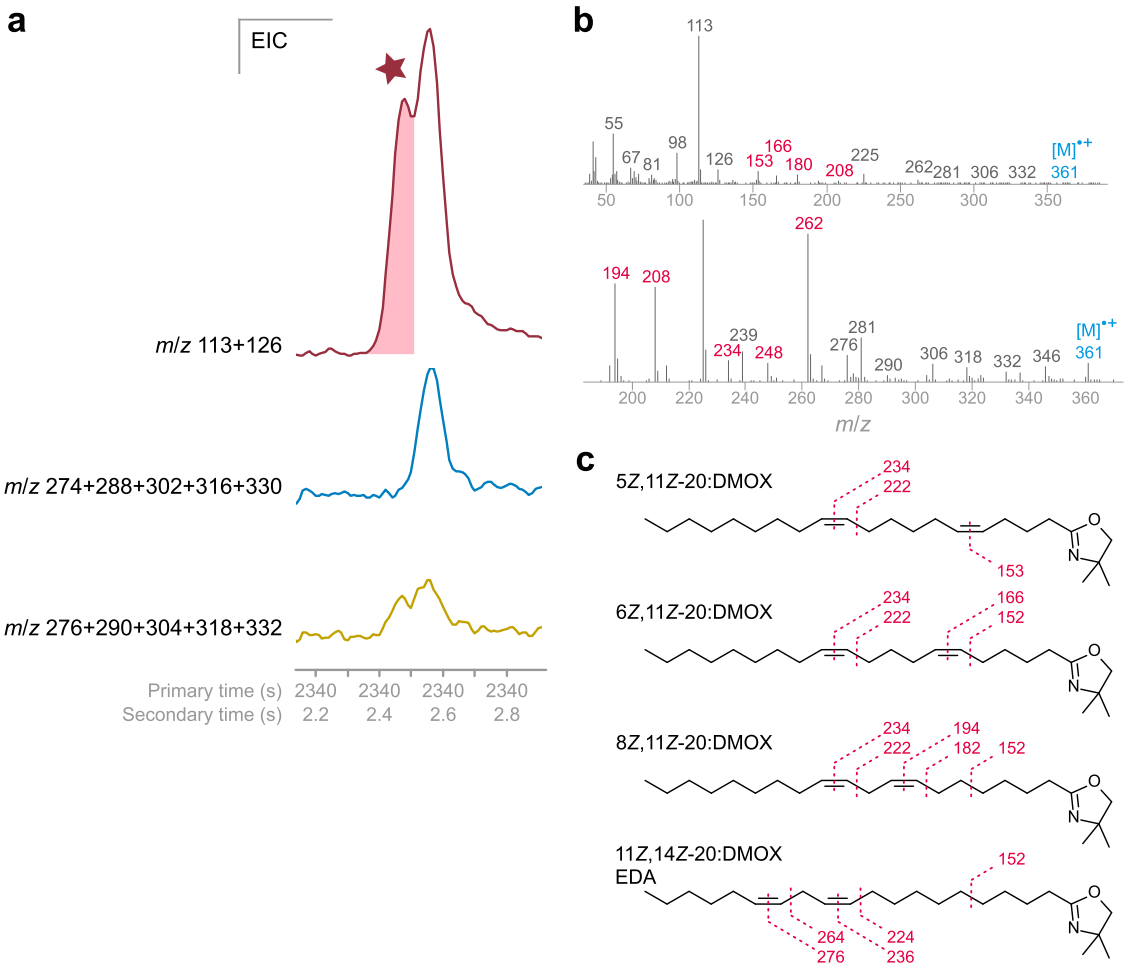

Supplementary Figure 22. Tentative identification of dienoic C20 FA in termite. **a** Selected sections of extracted ion chromatograms of AMP-derivatized total lipid extract from *P. simplex* workers (carcasses). A star indicates the unidentified 20:2 peak. **b** Mass spectrum (*top*: spectrum, *bottom*: spectrum zoomed at lower-abundance *m*/*z* region) of unidentified 20:2 FA eluting close to ScA. The data were acquired using GC×GC-MS. **c** A plausible structure of the unidentified 20:2 FA inferred from its mass spectrum and the reference structures of similar (6*Z*,11*Z*-20:) and less similar (8*Z*,11*Z*-20:, EDA) dienoic FAs. The main diagnostic ions arising theoretically from 5,11-, 6,11-, 8,11- and 11,14-diunsaturated systems are shown on the respective structures. To compare, see Supplementary Fig. 19d for the mass spectrum of a DMOX derivative of EDA detected in termite tissue.

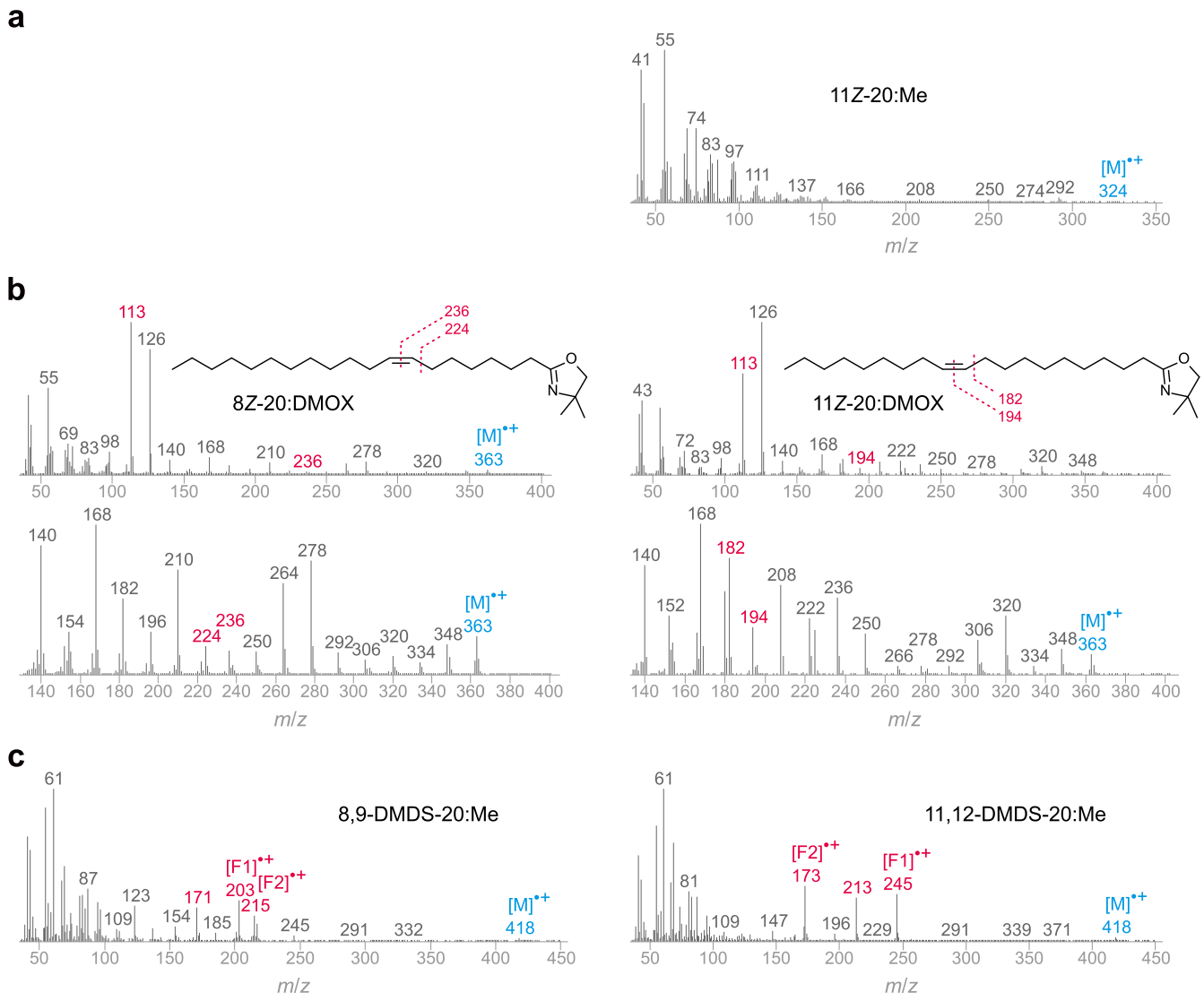

Supplementary Figure 23. Mass spectrometric characterization of C20 MUFAs in termite. a–c Mass spectra of major monounsaturated C20 FAs detected in *P. simplex* workers (carcasses) total lipid extracts (*left*: 8-unsaturated, *right*: 11-unsaturated) as FAMEs (**a**) and upon forming DMOX (**b**) and DMDS (**c**) derivatives. The intact spectrum of 8*Z*-20:Me could not be unambiguously retrieved because of coelution with EDA and 11*Z*-20:. The diagnostic ions of DMDS adducts are denoted analogously to those in Supplementary Fig. 4. The data were acquired using GC×GC-MS.

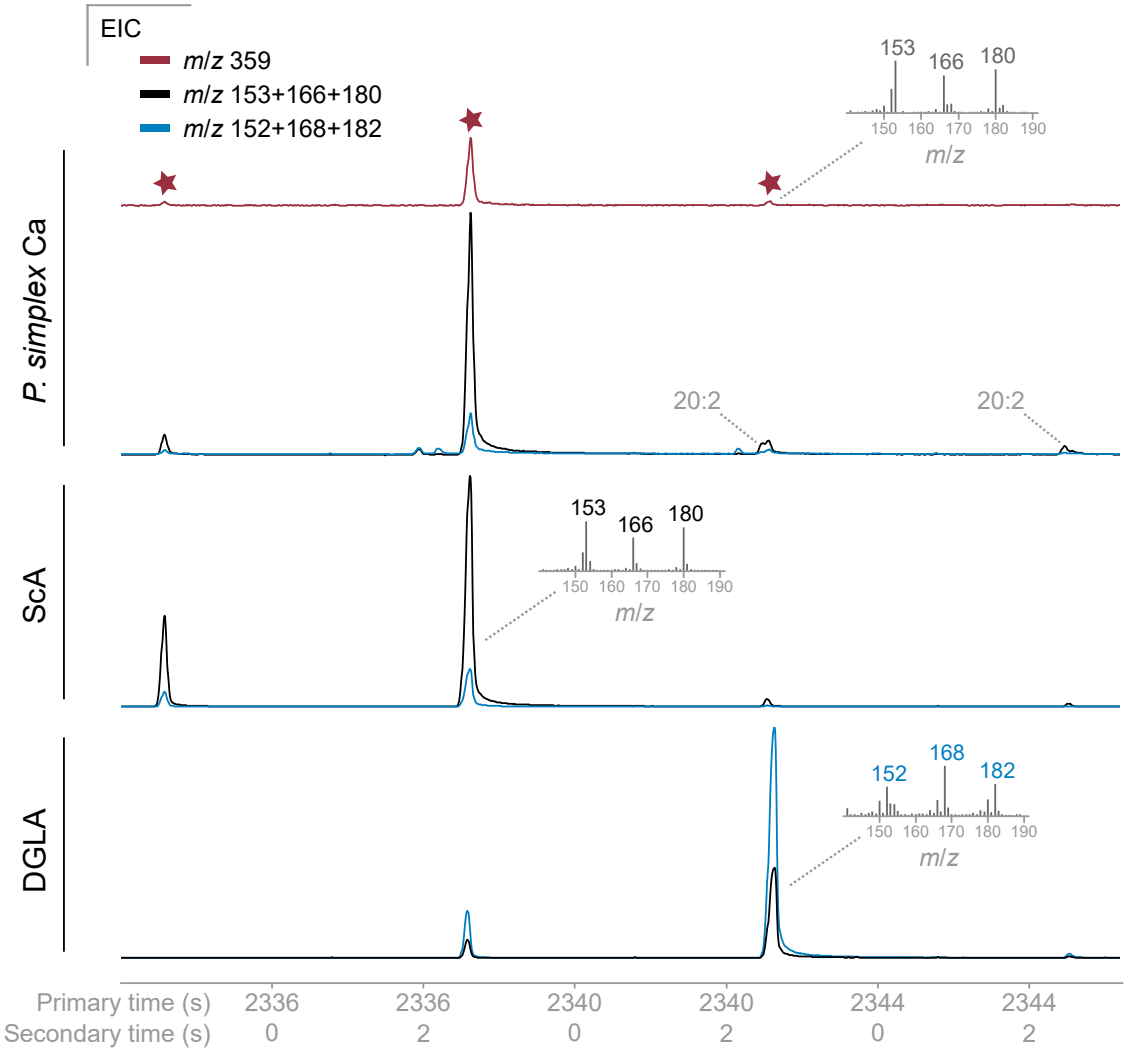

Supplementary Figure 24. Trienoic C20 FAs in termite. Partial extracted ion chromatograms of AMP-derivatized total lipid extract from *P. simplex* workers (carcasses) and standards of sciadonic acid (ScA) and dihomo-γ-linolenic acid (DGLA), including mass spectra of selected peaks focused on distinct *m*/*z* region. The 20:3 DMOX derivatives (based on *m*/*z* 359) detected in *P. simplex* extract are indicated by stars. The peaks of unidentified 20:2 (likely 5*Z*,11*Z*-20:) eluting just before 20:3 are indicated. The 5,11,14- and 8,11,14-triunsaturated systems are visualized using *m*/*z* of 153+166+180 and 152+168+182, respectively. The data were acquired using GC×GC-MS.

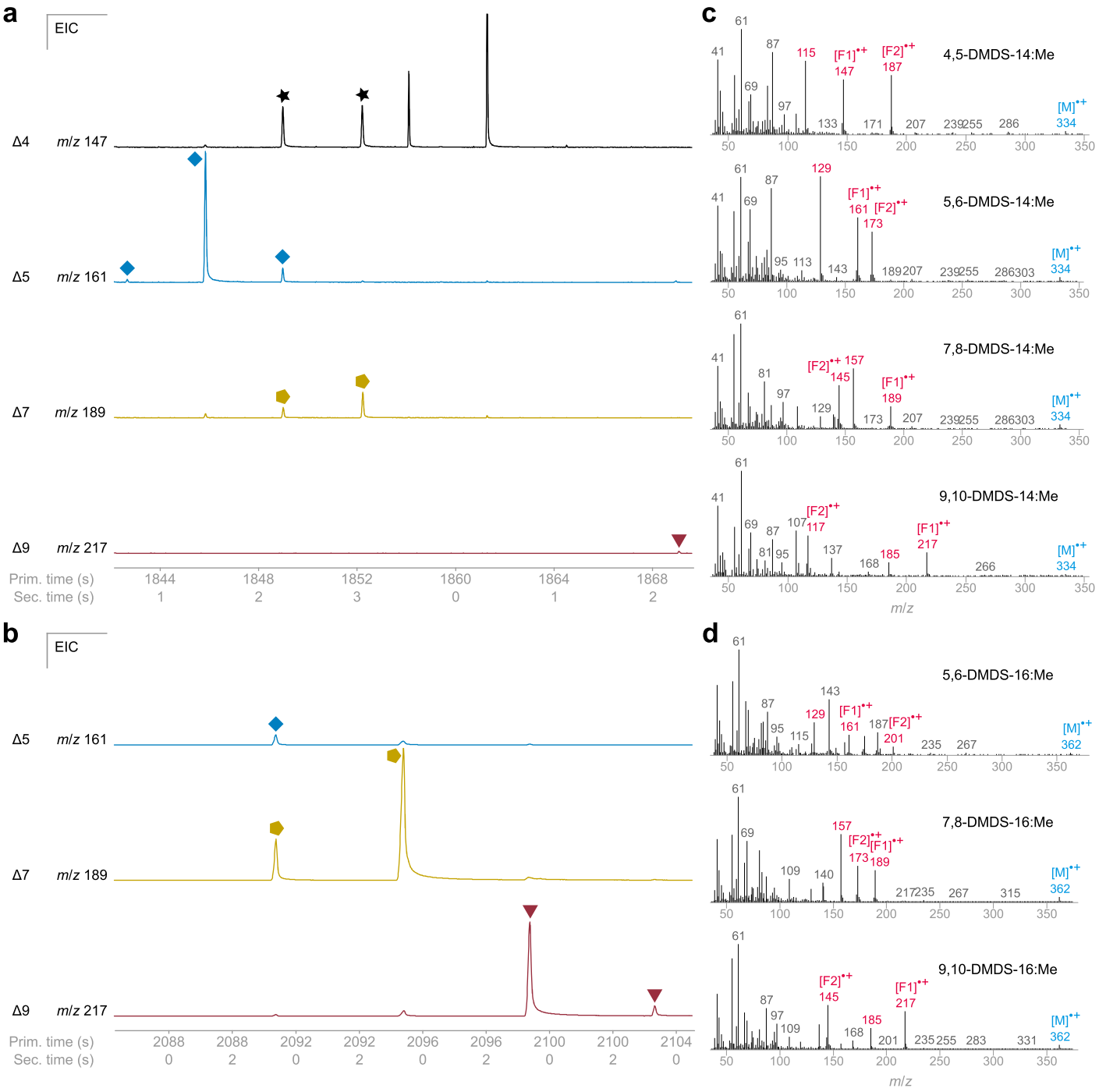

Supplementary Figure 25. Monounsaturated C14 and C16 FAs in termite. ab Selected sections of extracted ion chromatograms of DMDS-derivatized total lipid extract from *P. simplex* workers (carcasses) depicting C14 (**a**) and C16 (**b**) MUFA region. The 4,5-DMDS (stars), 5,6-DMDS (rectangles), 7,8-DMDS (pentagons) and 9,10-DMDS (triangles) adducts are visualized using *m*/*z* of 147, 161, 189 and 217, respectively. **cd** Mass spectra of major monounsaturated C14 (**c**) and C16 (**d**) FAs detected in *P. simplex* workers (carcasses) total lipid extracts upon DMDS derivatization. The diagnostic ions are indicated analogously to those in Supplementary Fig. 4. The data were acquired using GC×GC-MS.

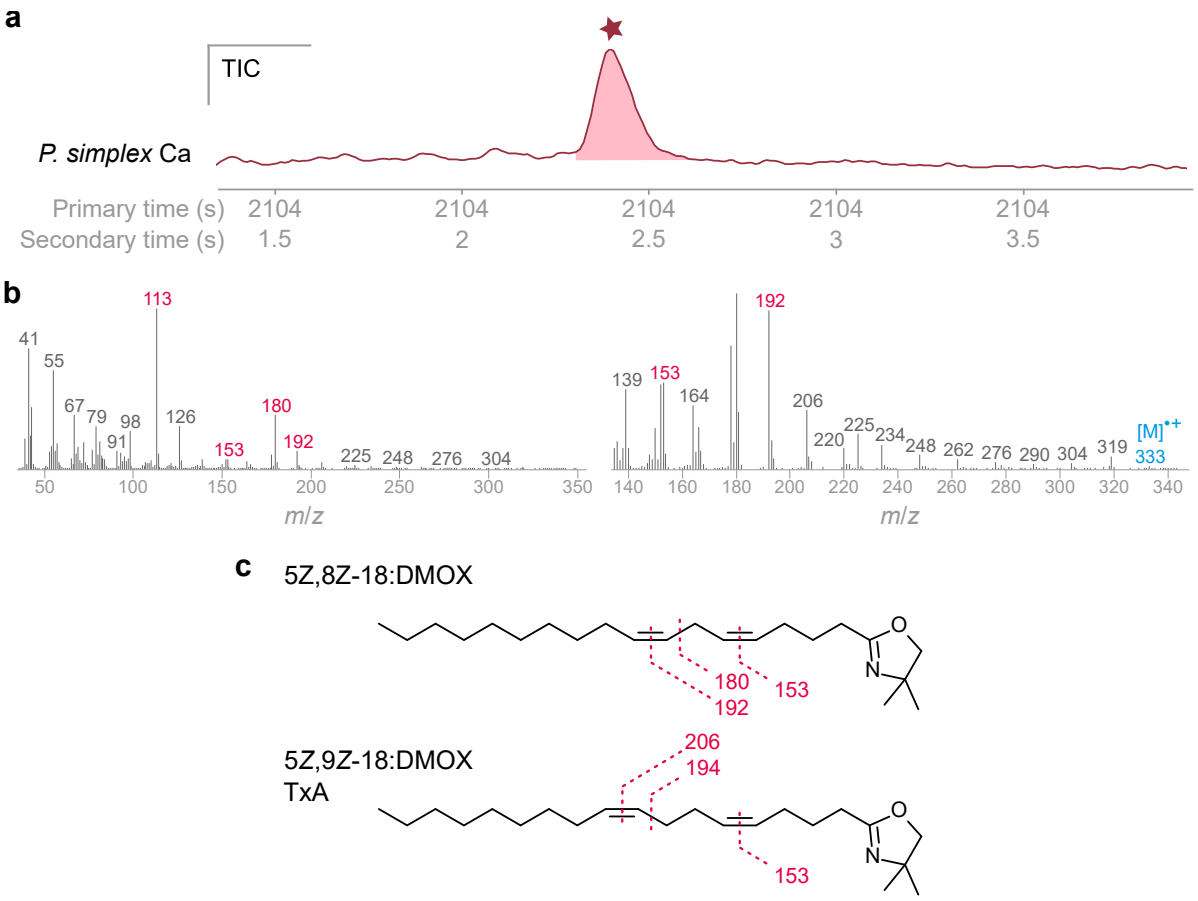

Supplementary Figure 26. Tentative identification of dienoic C18 FA in termite. **a** Selected sections of total ion chromatogram of AMP-derivatized total lipid extract from *P. simplex* workers (carcasses). A star indicates the unidentified 18:2 peak. **b** Mass spectrum (*left*: spectrum, *right*: spectrum zoomed at lower-abundance *m*/*z* region) of 18:2 peak. The data were acquired using GC×GC-MS. **c** A plausible structure of the unidentified 18:2 FA inferred from its mass spectrum and the reference structure of similar taxoleic acid (TxA). The main diagnostic ions arising theoretically from 5,8- and 5,9-diunsaturated systems are shown.

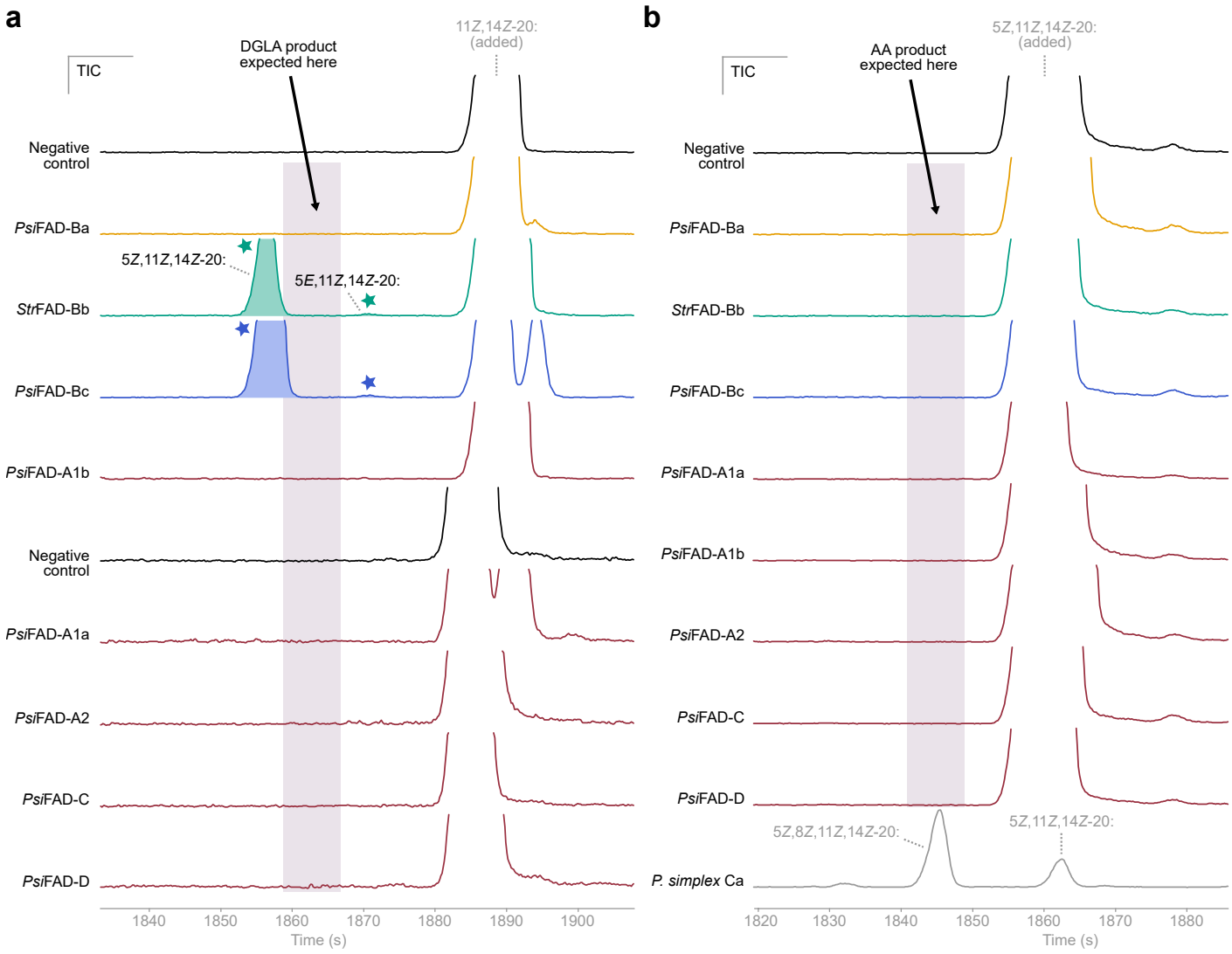

Supplementary Figure 27. Screening for △8 conversion of eicosadienoic and sciadonic acid by termite FADs. ab Selected sections of total ion chromatograms of FAME extracts from yeast expressing termite SCD-like FADs[1] supplemented with EDA (**a**) or ScA (**b**) and of FAME extract from *P. simplex* workers (carcasses). Stars indicate the FAD specific products deriving from EDA. The data were acquired using GC-MS.

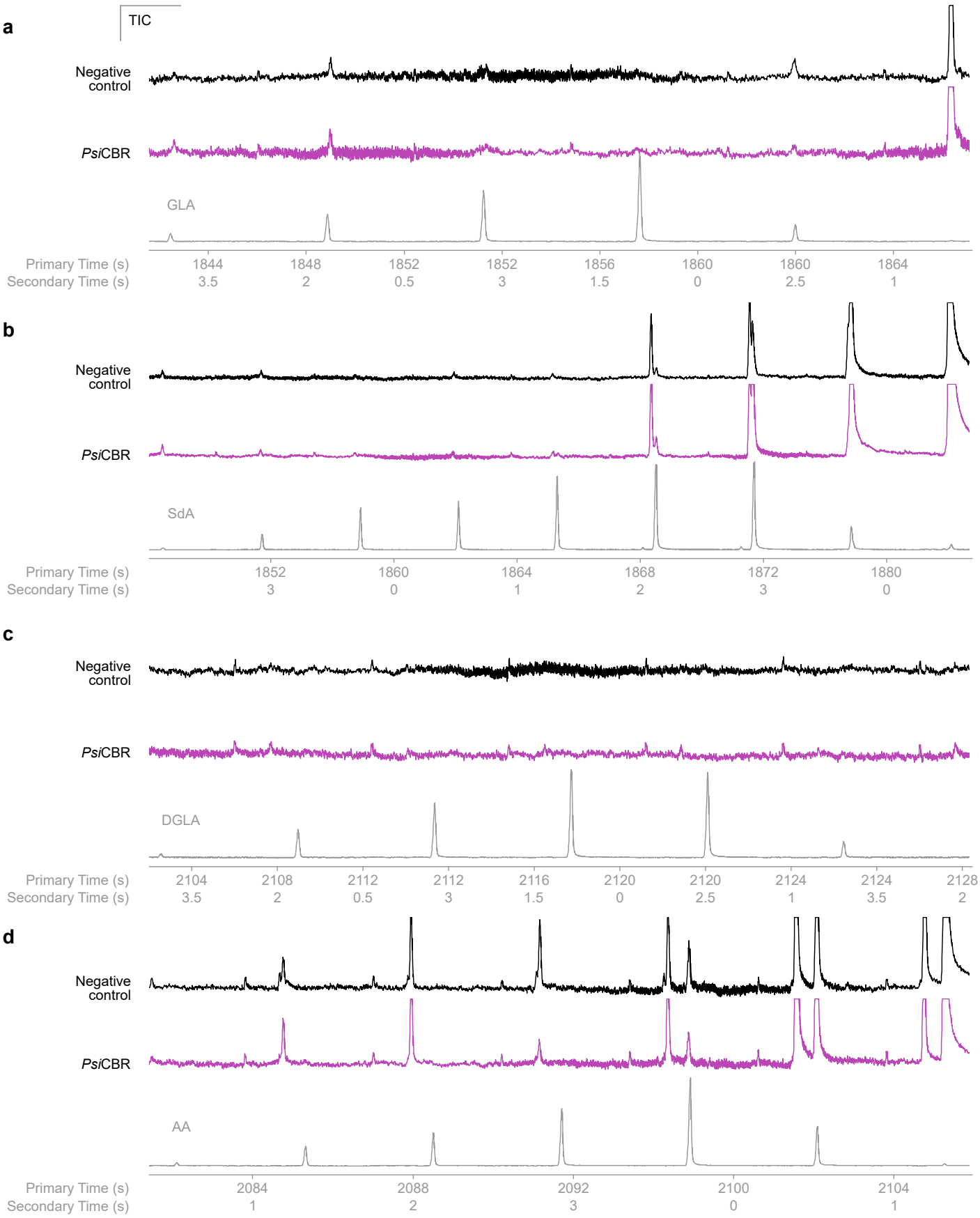

Supplementary Figure 28. Screening for △6 or △8 conversion of PUFAs by termite CBR protein. a–d Selected sections of total ion chromatograms of FAME extracts from yeast expressing *Psi*CBR supplemented with LA (**a**), ALA (**b**), EDA (**c**), or ScA (**d**), and of FAME standards of the expected products: GLA (**a**), stearidonic acid (SdA, **b**), DGLA (**c**), and AA (**d**). The data were acquired using GC×GC-MS.

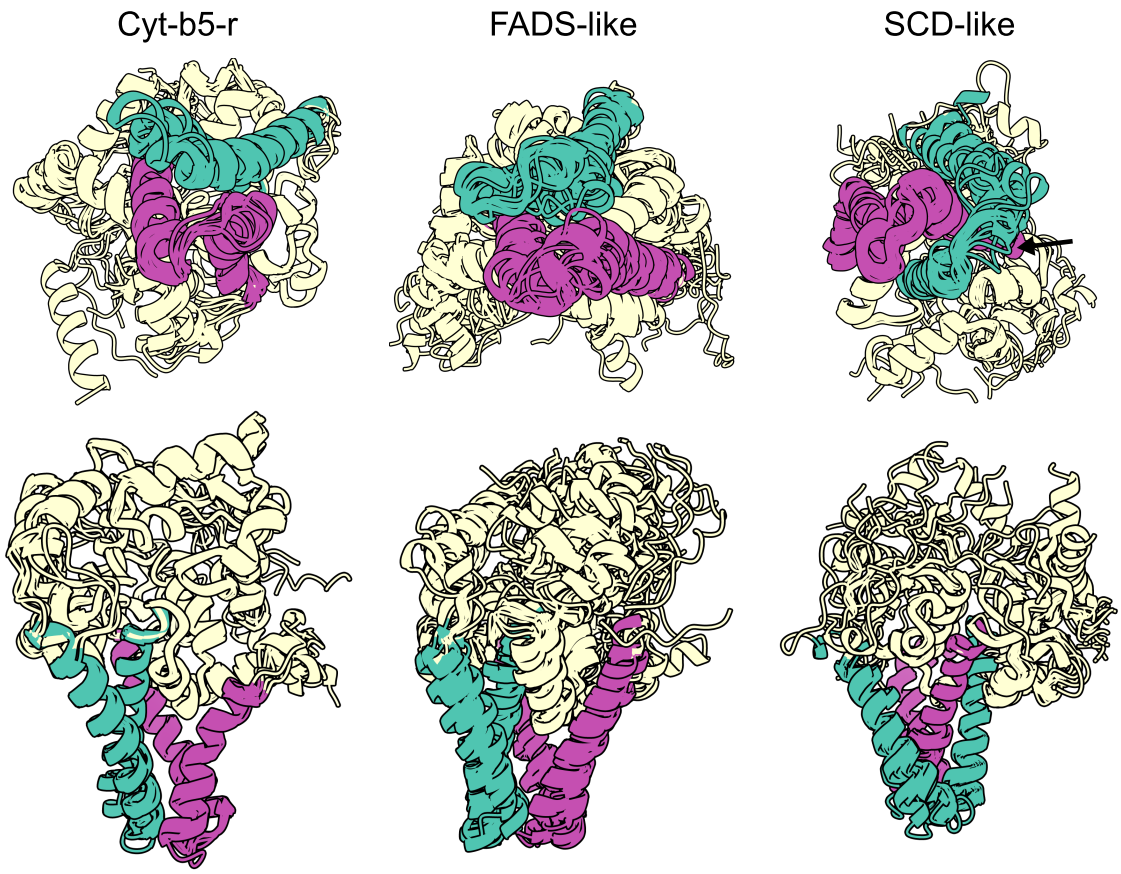

Supplementary Figure 29. Divergent positioning of transmembrane helices in Cyt-b5-r proteins and desaturases. Aligned AlphaFold-generated models of insect CBR proteins (7 models) and eukaryotic FADS-like (14 models) and SCD-like (13 models, 1 X-ray structure) desaturases, as viewed from ER lumen (*top*) and in parallel with membrane (*bottom*). The first two transmembrane (TM) helices (1 and 2; protein sequence-wise) are colored green, while the second two TM helices (3 and 4) are colored violet. A black arrow points at the TM helix 4 partially protruding from between TM helices 1 and 2. CBR models: *Aedes aegypti* (AlphaFold PSD accession number Q178Y2), *Drosophila melanogaster* (P19967), *Nasonia vitripennis* (A0A7M6UVL0), *P. simplex* CBR (in-house), *Spodoptera exigua* (A0A1V0M867), *Tribolium castaneum* (D6WVJ1), *Timema douglasi* (A0A7R8VR31). FADS-like models: *Caenorhabditis elegans* FAT4 (G5EG11), *Chlamydomonas reinhardtii* (Q2HWK7), *Danio rerio* FADS2 (Q9DEX7), *Tigriopus californicus* Fed5 (in-house), human FASDS1 and FADS2 (O60427 and O95864), *Mortierella alpina* (in-house), *Octopus vulgaris* Des (G1EN35), *Rebecca salina* D5Des (A4KDP0), *Siganus canaliculatus* Fad1 and Fad2 (in-house), *Salmo salar* Fadsd5 (Q8QGE2), *Torreya grandis* DES1 (in-house), *Thraustochytrium* FAD5 (Q8S3C1). SCD-like models: *Anemone leveillei* AL21 (P0DOW3), *Bombyx mori* (in-house), *Bombus terrestris* SPVE (in-house), *Ctenopseustis obliquana* desat7 (in-house), mouse SCD1 (PDB 4YMK), *Manduca sexta* D3 (in-house), *N. vitripennis* XP_001607533 (in-house), Ostrinia nubilalis (in-house), Periplaneta americana FAD-A1b[1], *Planotortrix octo* (Q95UU3), *P. simplex* FAD-Bc (in-house), *Saccharomyces cerevisiae* OLE1 (P21147), *T. castaneum* D12Des[1], *Trichoplusia ni* (in-house). See Supplementary Table 1 for remaining accession numbers.

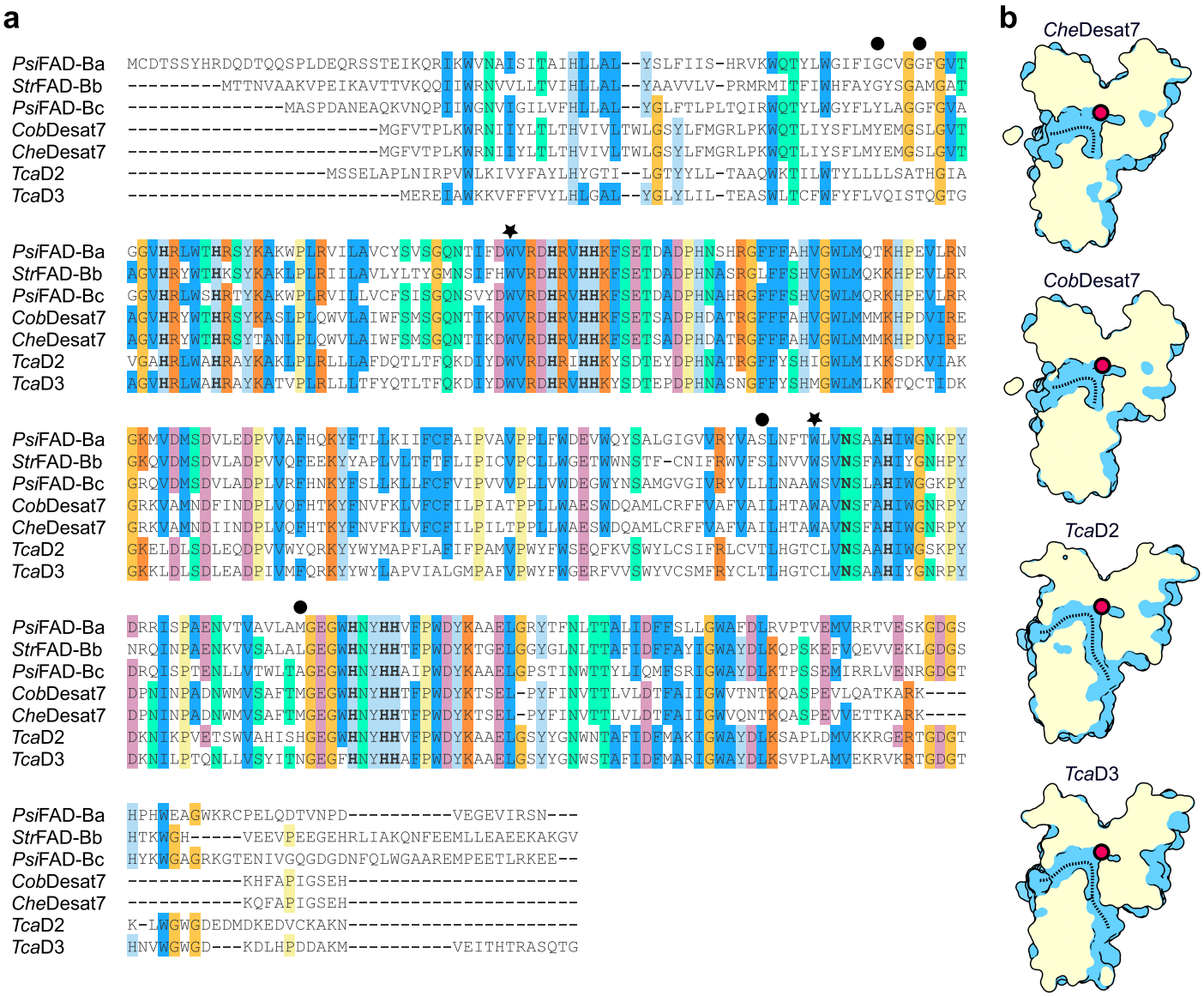

Supplementary Figure 30. Comparison of insect △5 desaturases. a A multiple sequence alignment of termite FAD-Bs and functionally characterized △5 desaturases from lepidopterans (Desat7s from *Ctenopseustis obliquana* and *C. herana*)[5] and beetle (D2 and D3 from *Tribolium castaneum*)[6]. The positions of residues which could participate in binding of the C_1 acyl moiety of the FA substrate are indicated by stars. The positions of residues which may modulate the substrate tunnel architecture due to steric reasons, based on inspection of AlphaFold-generated models, are indicated by dots. The conserved metal ion-binding active site residues are depicted in bold. **b** Cross-sections of AlphaFold-generated models of lepidopteran and beetle △5 desaturases. The protein surface (internal and external) is colored blue, and the substrate tunnel shape and length are indicated using a dashed line. The active site is shown as a red circle. Predicted models are provided in Supplementary Data 2.

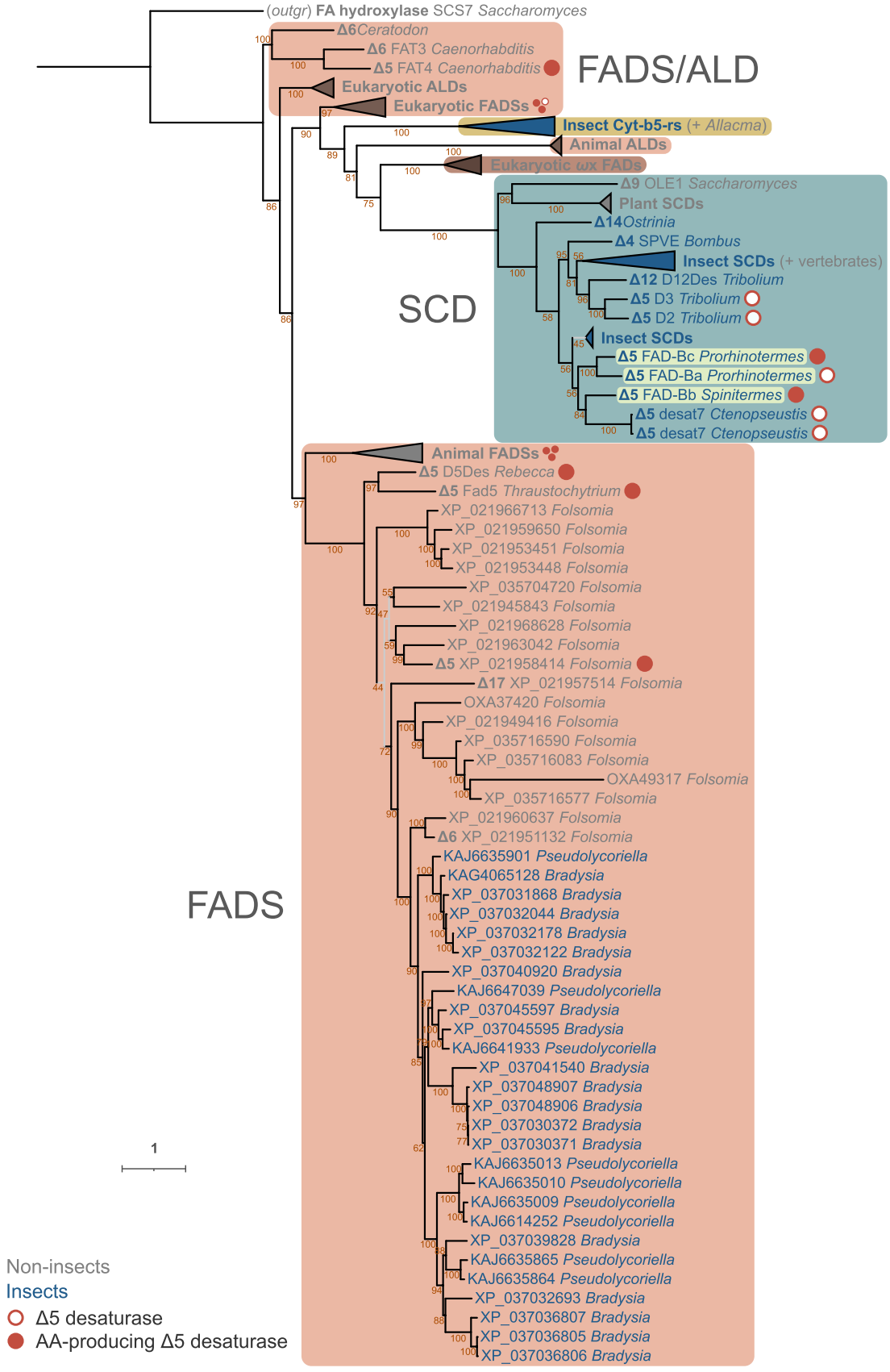

Supplementary Figure 31. Phylogeny of collembolan and dipteran FADS-like desaturases. A phylogenetic tree of the same desaturases and related proteins as in Fig. 6, additionally including putative FADS-like desaturases from springtails (Entomobryomorpha: Isotomidae; *Folsomia candida*)[3], and from dark-winged fungus gnats (Diptera: Sciaridae; *Bradysia coprophila*, *B. odoriphaga*, *Pseudolycoriella hygida*). Large branches are collapsed for clarity. Termite FADs functionally characterized in this study are shown on green background. Proteins from *F. candida* which have been recently functionally characterized as Δ5, Δ6 and Δ17 desaturases[4] are indicated. The branching with bootstrap support <50 is colored grey. If not shown directly, the accession numbers are listed in Supplementary Table 1.

Supplementary Table 1. The list of protein sequences used to generate Fig. 6. N.S. stands for not specified.

Name	Regiospecificity	Organism	Accession number	Reference
Cyt-b5-r	N.S.	*Acanthoscelides obtectus*	CAH2010246	Retrieved from UniProt
N.S.	ω3	*Acropora millepora*	ATV93523	7
ωx1	ω3	*Adineta vaga*	ATV93531	7
Cyt-b5-r	N.S.	*Aedes aegypti*	EAT42760	Retrieved from UniProt
D12Des	Δ12	*Acheta domesticus*	ABY26957	8
D9Des	Δ9	*Acheta domesticus*	AAK25796	8
Cyt-b5-r	N.S.	*Allacma fusca*	CAG7727030	Retrieved from UniProt
AL10	Δ5	*Anemone leveillei*	P0DOW2	9
AL21	Δ5	*Anemone leveillei*	P0DOW3	9
PGΔ6	Δ6	*Antheraea pernyi*	ADO85597	10
N.S.	Δ8(sphingolipid)	*Arabidopsis thaliana*	CAA11858	11
FAD2	ω6	*Arabidopsis thaliana*	AAA32782	12
ADS2	ω9	*Arabidopsis thaliana*	OAP08999	13
Cyt-b5-r	N.S.	*Athalia rosae*	XP_012254794	Retrieved from UniProt
FADS2	Δ5/Δ6/Δ8	*Barbonymus gonionotus*	AXF92413	14
FAD2-9	Δ12	*Bemisia tabaci*	WQH19958	15
Cyt-b5-r	N.S.	*Bicyclus anynana*	XP_052740595	Retrieved from UniProt
Cyt-b5-r	N.S.	*Blattella germanica*	PSN40733	Retrieved from UniProt
FAD-B	Δ5	*Bombus terrestris*	XP_012169975	This work
NPVE	Δ9	*Bombus terrestris*	CAW34805	16
SPVE	Δ4	*Bombus terrestris*	AGK82078	16
Cyt-b5-r	N.S.	*Bombus terrestris*	XP_003397478	Retrieved from NCBI
N.S.	N.S.	*Bombus terrestris*	XP_003402131	Retrieved from NCBI
desat1	Δ11/conjugase	*Bombyx mori*	BAD18122	17
Cyt-b5-r	Δ6	*Bombyx mori*	XP_012544041	18
Cyt-b5-r	N.S.	*Bombyx mori*	XP_004924008	Retrieved from NCBI
N.S.	Δ6	*Borago officinalis*	AAC49700	11
N.S.	Δ8(sphingolipid)	*Borago officinalis*	AAG43277	19
N.S.	Δ8(sphingolipid)	*Brassica napus*	CAA11857	11
FAT4	Δ5	*Caenorhabditis elegans*	AAC95143	20
FAT1	ω3	*Caenorhabditis elegans*	AAA67369	20
FAT3	Δ6	*Caenorhabditis elegans*	AAC15586	20
FAT2	Δ^{+3} (Δ12/Δ15)	*Caenorhabditis elegans*	AAF63745	20
N.S.	Δ6	*Ceratodon purpureus*	CAB94993	21
CL10	Δ12/acetylenase	*Chauliognathus lugubris*	AFJ66832	22
DES	ω13 (Δ5/Δ7)	*Chlamydomonas reinhardtii*	BAE79428	23
Z/E11	Δ11	*Choristoneura rosaceana*	AAN41250	24
Cyt-b5-r	N.S.	*Coptotermes formosanus*	GFG35478	Retrieved from UniProt
Cyt-b5-r	N.S.	*Cryptotermes secundus*	XP_023723742	Retrieved from UniProt
Desat7	Δ5	*Ctenopseustis herana*	AHB33601	5
Desat7	Δ5	*Ctenopseustis obliquana*	AHB33599	5
CPRQ	Δ9/conjugase	*Cydia pomonella*	AHW98354	25
FADS2	Δ6/Δ5	*Danio rerio*	AAG25710	26
Cyt-b5-r	N.S.	*Dendroctonus ponderosae*	ENN71160	Retrieved from UniProt
fadA	Δ5	*Dictyostelium discoideum*	BAA81814	27
IFC	Δ4(sphingolipid)	*Drosophila melanogaster*	AAL28744	28
Cyt-b5-r	N.S.	*Drosophila melanogaster*	AAL13516	29
FAD-A1a	Δ9	*Embiratermes neotenicus*	WGF20538	1
FAD-A1b	Δ12	*Embiratermes neotenicus*	WGF20537	1
Δ12L	Δ12	*Folsomia candida*	XP_021946727	4
Δ5	Δ5	*Folsomia candida*	XP_021958414	4
Δ6	Δ6	*Folsomia candida*	XP_021951132	4
Δ17L	Δ17	*Folsomia candida*	XP_021957514	4

Supplementary Table 1. (*continued*)

Name	Regiospecificity	Organism	Accession number	Reference
Cyt-b5-r	N.S.	*Folsomia candida*	XP_021956929	Retrieved from NCBI
Cyt-b5-r	N.S.	*Folsomia candida*	XP_021948429	Retrieved from NCBI
Cyt-b5-r	N.S.	*Folsomia candida*	XP_021960367	Retrieved from NCBI
Cyt-b5-r	N.S.	*Folsomia candida*	XP_021959864	Retrieved from NCBI
Cyt-b5-r	N.S.	*Folsomia candida*	XP_021967112	Retrieved from NCBI
D5	Δ5	*Globisporangium irregulare*	AAL13311	30
Cyt-b5-r	N.S.	*Helicoverpa zea*	XP_047022646	Retrieved from UniProt
FADS1	Δ5	*Homo sapiens*	O60427	31
FADS2	Δ6	*Homo sapiens*	AAD20018	32
DEGS1	Δ4(sphingolipid)	*Homo sapiens*	AAH00961	28
SCD1	Δ9	*Homo sapiens*	CAA73998	33
FAD-B	Δ5	*Ischnura elegans*	XP_046405721	This work
Cyt-b5-r	N.S.	*Ischnura elegans*	XP_046396474	Retrieved from UniProt
N.S.	N.S.	*Ischnura elegans*	XP_046383437	Retrieved from NCBI
N.S.	N.S.	*Ischnura elegans*	XP_046383434	Retrieved from NCBI
N.S.	Δ8(sphingolipid)	*Kluyveromyces lactis*	BAB93118	34
N.S.	Δ8(sphingolipid)	*Lachancea kluyveri*	BAB93117	34
N.S.	ω3	*Lepeophtheirus salmonis*	ATV93526	7
N.S.	Δ5	*Limnanthes douglasii*	AAG28599	35
D2	Δ11/conjugase	*Manduca sexta*	CAJ27976	36
D3	Δ14	*Manduca sexta*	CAJ43430	36
Cyt-b5-r	N.S.	*Manduca sexta*	XP_030041312	Retrieved from UniProt
DES5	Δ5	*Marchantia polymorpha*	AAT85663	37
VFAD	ω8/ω9	*Marchantia polymorpha*	PTQ48035	38
DES1	Δ5	*Mortierella alpina*	AAC39508	39
SCD1	Δ9	*Mus musculus*	NP_033153	40
FAD-Ba	Δ5	*Myzus persicae*	XP_022168642	This work
N.S.	N.S.	*Myzus persicae*	XP_022164670	Retrieved from NCBI
Cyt-b5-r	N.S.	*Myzus persicae*	XP_022176544	Retrieved from NCBI
Cyt-b5-r	N.S.	*Myzus persicae*	XP_022171429	Retrieved from NCBI
D12a	Δ12	*Nasonia vitripennis*	XP_001599836	41
Cyt-b5-r	N.S.	*Nasonia vitripennis*	NP_001136324	Retrieved from UniProt
Fad	Δ5	*Octopus vulgaris*	AEK20864	42
N.S.	Δ14	*Ostrinia nubilalis*	AAL35330	43
Cyt-b5-r	N.S.	*Ostrinia nubilalis*	XP_063824542	Retrieved from UniProt
FADS1	Δ5	*Papio anubis*	ABP06289	44
FADS2	ω12 (Δ6/Δ8)	*Papio anubis*	ACI46980	45
FadsA	Δ5	*Paracentrotus lividus*	AQP31155	46
FadsC1	Δ8	*Paracentrotus lividus*	AQP31156	46
FadsC2	Δ8	*Paracentrotus lividus*	AQP31157	46
N.S.	ω3	*Patella vulgata*	ATV93528	7
FAD-A1a	Δ9	*Periplaneta americana*	WGF20534	1
FAD-A1b	Δ12/Δ11	*Periplaneta americana*	WGF20533	1
D5	Δ5	*Phaeodactylum tricornutum*	ABP65280	47
DES5	Δ5	*Physcomitrium patens*	CAI58861	48
SFD	ω8/ω9	*Physcomitrium patens*	XP_024359978	13
VFAD2	ω8/ω9	*Physcomitrium patens*	XP_024402076	38
FAD5	Δ5	*Phytophthora megasperma*	CAD53323	49
Cyt-b5-r	N.S.	*Pieris rapae*	XP_022125794	Retrieved from UniProt
Z9	Δ9	*Planotortrix octo*	AAF73073	50
Z10	Δ10	*Planotortrix octo*	AAG54077	50
N.S.	ω3	*Platynereis dumerilii*	ATV93530	7
FAD-Ba	Δ5	*Plutella xylostella*	XP_011550250	This work

Supplementary Table 1. (*continued*)

Name	Regiospecificity	Organism	Accession number	Reference
Cyt-b5-r	N.S.	*Plutella xylostella*	XP_011550465	Retrieved from UniProt
N.S.	N.S.	*Plutella xylostella*	XP_048488081	Retrieved from NCBI
N.S.	N.S.	*Prorhinotermes simplex*	GASE02046388	Retrieved from NCBI
CBR	N.S.	*Prorhinotermes simplex*	PQ181303	This work
FAD-Ba	Δ5	*Prorhinotermes simplex*	WGG88805	This work; 1
FAD-Bc	Δ5	*Prorhinotermes simplex*	WGG88808	This work; 1
FAD-A1a	Δ9	*Prorhinotermes simplex*	WGG88803	1
FAD-A1b	Δ12	*Prorhinotermes simplex*	WGG88804	1
FADS1	Δ5	*Rattus norvegicus*	AAG35068	51
FADS2	Δ6	*Rattus norvegicus*	BAA75496	52
FADS3	Δ13/Δ14	*Rattus norvegicus*	CAD38527	53
D5Des	Δ5	*Rebecca salina*	ABL96295	54
SCS7	N.S.	*Saccharomyces cerevisiae*	CAA89255	55
OLE1	Δ9	*Saccharomyces cerevisiae*	AAA34826	56
Fadsd5	Δ5	*Salmo salar*	AAL82631	57
Fads1	Δ5	*Scyliorhinus canicula*	AEY94454	58
Fads2	Δ6	*Scyliorhinus canicula*	AEY94455	58
Fad	Δ5	*Sepia officinalis*	AKE92955	59
Cyt-b5-r	N.S.	*Schistocerca nitens*	XP_049801995	Retrieved from UniProt
FAD2	Δ4/Δ5	*Siganus canaliculatus*	ADJ29913	60
FAD1	Δ6/Δ5	*Siganus canaliculatus*	ABR12315	60
FAD-Bb	Δ5	*Spinitermes trispinosus*	WGG88822	This work; 1
N.S.	Δ11/Δ12	*Spodoptera exigua*	ARD71181	61
IFC	Unknown	*Spodoptera exigua*	ARD71182	Retrieved from UniProt
Cyt-b5-r	N.S.	*Spodoptera exigua*	ARD71179	Retrieved from UniProt
Cyt-b5-r	N.S.	*Spodoptera exigua*	ARD71184	Retrieved from UniProt
FL3	Δ11	*Spodoptera littoralis*	AAQ74259	62
Cyt-b5-r	N.S.	*Tenebrio molitor*	CAH1383251	Retrieved from UniProt
Fad5	Δ5	*Thraustochytrium*	AAM09687	63
Fad4	Δ4	*Thraustochytrium*	AAM09688	63
Fed5	Δ5	*Tigriopus californicus*	QWC69498	64
Fed1	Δ6	*Tigriopus californicus*	QWC69494	64
ωx2	$\Delta 9/\Delta^{+3}$	*Tigriopus californicus*	QWC69500	64
Fed2	Δ4	*Tigriopus californicus*	QWC69495	64
Fed3	ω12 (Δ6/Δ8)	*Tigriopus californicus*	QWC69496	64
Cyt-b5-r	N.S.	*Timema douglasi*	CAD7201058	Retrieved from UniProt
DES1	Δ5	*Torreya grandis*	TG9g01925	65
D2	Δ5	*Tribolium castaneum*	NP_001306195	6
D3	Δ5	*Tribolium castaneum*	NP_001306194	6
D12Des	Δ12	*Tribolium castaneum*	ABY26958	8
D9DesA	Δ9	*Tribolium castaneum*	NP_001182164	8
N.S.	N.S.	*Tribolium castaneum*	XP_972076	Retrieved from NCBI
Cyt-b5-r	N.S.	*Tribolium castaneum*	XP_008196500	Retrieved from UniProt
PDesat	Δ11	*Trichoplusia ni*	AAD03775	66
Cyt-b5-r	N.S.	*Zootermopsis nevadensis*	XP_021916980	Retrieved from UniProt
FAD-A1a	Δ9	*Zootermopsis nevadensis*	WGF20536	1
FAD-A1b	Δ12	*Zootermopsis nevadensis*	WGF20535	1
Cyt-b5-r	N.S.	*Zophobas morio*	XP_063904262	Retrieved from UniProt

Supplementary References

1. Macháček, S. *et al.* Evolution of Linoleic Acid Biosynthesis Paved the Way for Ecological Success of Termites. *Mol. Biol. Evol.* **40**, msad087 (2023). https://doi.org/10.1093/molbev/msad087.

2. Knipple, D. C., Rosenfield, C. L., Nielsen, R., You, K. M. & Jeong, S. E. Evolution of the integral membrane desaturase gene family in moths and flies. *Genetics* **162**, 1737–1752 (2002). https://doi.org/10.1093/genetics/162.4.1737.

3. Menzel, R., Tobias, K., Fidan, T., Rietz, A. & Ruess, L. Dissection of the synthesis of polyunsaturated fatty acids in nematodes and Collembola of the soil fauna. *Biochim. Biophys. Acta Mol. Cell Biol. Lipids* **1869** (2024). https://doi.org/10.1016/j.bbalip.2024.159541.

4. Ohhara, Y., Sato, A., Hirono-Hara, Y., Hara, K. Y. & Yamakawa-Kobayashi, K. Evolution of a horizontally acquired fatty acid desaturase enables the biosynthesis of ω-3 polyunsaturated fatty acids in Collembola. *Insect Biochem. Mol. Biol.* **183** (2025). https://doi.org/10.1016/j.ibmb.2025.104381.

5. Hagström, Å. K. *et al.* A Novel Fatty Acyl Desaturase from the Pheromone Glands of *Ctenopseustis obliquana* and *C. herana* with Specific *Z*5-Desaturase Activity on Myristic Acid. *J. Chem. Ecol.* **40**, 63–70 (2014). https://doi.org/10.1007/s10886-013-0373-1.

6. Haritos, V. S., Home, I., Damcevski, K., Glover, K. & Gibb, N. Unexpected functional diversity in the fatty acid desaturases of the flour beetle *Tribolium castaneum* and identification of key residues determining activity. *Insect Biochem. Mol. Biol.* **51**, 62–70 (2014). https://doi.org/10.1016/j.ibmb.2014.05.006.

7. Kabeya, N. *et al.* Genes for de novo biosynthesis of omega-3 polyunsaturated fatty acids are widespread in animals. *Sci. Adv.* **4**, eaar6849 (2018). https://doi.org/10.1126/sciadv.aar6849.

8. Zhou, X. R. *et al.* Isolation and functional characterization of two independently-evolved fatty acid △12-desaturase genes from insects. *Insect Mol. Biol.* **17**, 667–676 (2008). https://doi.org/10.1111/j.1365-2583.2008.00841.x.

9. Sayanova, O., Haslam, R., Caleron, M. V. & Napier, J. A. Cloning and characterization of unusual fatty acid desaturases from *Anemone leveillei*: Identification of an acyl-coenzyme A C_{20} Δ^5-desaturase responsible for the synthesis of sciadonic acid. *Plant. Physiol.* **144**, 455–467 (2007). https://doi.org/10.1104/pp.107.098202.

10. Wang, H. L., Liénard, M. A., Zhao, C. H., Wang, C. Z. & Löfstedt, C. Neofunctionalization in an ancestral insect desaturase lineage led to rare Δ^6 pheromone signals in the Chinese tussah silkworm. *Insect Biochem. Mol. Biol.* **40**, 742–751 (2010). https://doi.org/10.1016/j.ibmb.2010.07.009.

11. Sperling, P., Zähringer, U. & Heinz, E. A sphingolipid desaturase from higher plants. Identification of a new cytochrome b_5 fusion protein. *J. Biol. Chem.* **273**, 28590–28596 (1998). https://doi.org/10.1074/jbc.273.44.28590.

12. Covello, P. S. & Reed, D. W. Functional Expression of the Extraplastidial *Arabidopsis thaliana* Oleate Desaturase Gene (FAD2) in *Saccharomyces cerevisiae*. *Plant. Physiol.* **111**, 223–226 (1996). https://doi.org/10.1104/pp.111.1.223.

13. Resemann, H. C. *et al.* Convergence of sphingolipid desaturation across over 500 million years of plant evolution. *Nat. Plants* **7** (2021). https://doi.org/10.1038/s41477-020-00844-3.

14. Janaranjan, M. *et al.* Capacity for eicosapentaenoic acid and arachidonic acid biosynthesis in silver barb (*Barbonymus gonionotus*): Functional characterisation of a △6/△8/△5 Fads2 desaturase and Elovl5 elongase. *Aquaculture* **497**, 469–486 (2018). https://doi.org/10.1016/j.aquaculture.2018.08.019.

15. Gong, C. *et al.* A Horizontally Transferred Plant Fatty Acid Desaturase Gene Steers Whitefly Reproduction. *Adv. Sci.* **11**, e2306653 (2024). https://doi.org/10.1002/advs.202306653.

16. Buček, A. *et al.* The role of desaturases in the biosynthesis of marking pheromones in bumblebee males. *Insect Biochem. Mol. Biol.* **43**, 724–731 (2013). https://doi.org/10.1016/j.ibmb.2013.05.003.

17. Moto, K. *et al.* Involvement of a bifunctional fatty-acyl desaturase in the biosynthesis of the silkmoth, *Bombyx mori*, sex pheromone. *Proc. Natl. Acad. Sci. USA* **101**, 8631–8636 (2004). https://doi.org/10.1073/pnas.0402056101.

18. Yu, H.-Y., Zhou, Z.-F., Jia, J.-Q. & Gui, Z.-Z. Cloning, expression and functional analysis of a delta 6-desaturase gene from the silkworm, *Bombyx mori* L. *J. Asia-Pac. Entomol.* **19**, 581–587 (2016). https://doi.org/10.1016/j.aspen.2016.05.002.

19. Sperling, P., Libisch, B., Zähringer, U., Napier, J. A. & Heinz, E. Functional Identification of a Δ^8-Sphingolipid Desaturase from *Borago officinalis*. *Arch. Biochem. Biophys.* **388**, 293–298 (2001). https://doi.org/10.1006/abbi.2001.2308.

20. Watts, J. L. & Browse, J. Genetic dissection of polyunsaturated fatty acid synthesis in *Caenorhabditis elegans*. *Proc. Natl. Acad. Sci. USA* **99**, 5854–5859 (2002). https://doi.org/10.1073/pnas.092064799.

21. Sperling, P. *et al.* A bifunctional Δ^6-fatty acyl acetylenase/desaturase from the moss *Ceratodon purpureus*. *Eur. J. Biochem.* **267**, 3801–3811 (2000). https://doi.org/10.1046/j.1432-1327.2000.01418.x.

22. Haritos, V. S. *et al.* The convergent evolution of defensive polyacetylenic fatty acid biosynthesis genes in soldier beetles. *Nat. Commun.* **3**, 1150 (2012). https://doi.org/10.1038/ncomms2147.

23. Kajikawa, M. *et al.* A Front-end Desaturase from *Chlamydomonas reinhardtii* Produces Pinolenic and Coniferonic Acids by ω13 Desaturation in Methylotrophic Yeast and Tobacco. *Plant Cell Physiol.* **47**, 64–73 (2006). https://doi.org/10.1093/pcp/pci224.

24. Hao, G., O'Connor, M., Liu, W. & Roelofs, W. L. Characterization of Z/E11- and Z9-desaturases from the oblique-banded leafroller moth, *Choristoneura rosaceana*. *J. Insect Sci.* **2**, 26 (2002). https://doi.org/10.1093/jis/2.1.26.

25. Lassance, J. M., Ding, B. J. & Löfstedt, C. Evolution of the codling moth pheromone via an ancient gene duplication. *BMC Biol.* **19** (2021). https://doi.org/10.1186/s12915-021-01001-8.

26. Hastings, N. *et al.* A vertebrate fatty acid desaturase with Δ5 and Δ6 activities. *Proc. Natl. Acad. Sci. USA* **98**, 14304–14309 (2001). https://doi.org/10.1073/pnas.251516598.

27. Saito, T. & Ochiai, H. Identification of Δ^5-fatty acid desaturase from the cellular slime mold *Dictyostelium discoideum*. *Eur. J. Biochem.* **265**, 809–814 (1999). https://doi.org/10.1046/j.1432-1327.1999.00789.x.

28. Ternes, P., Franke, S., Zähringer, U., Sperling, P. & Heinz, E. Identification and characterization of a sphingolipid Δ4-desaturase family. *J. Biol. Chem.* **277**, 25512–25518 (2002). https://doi.org/10.1074/jbc.M202947200.

29. Levin, R. J., Boychuk, P. L., Croniger, C. M., Kazzaz, J. A. & Rozek, C. E. Structure and Expression of a Muscle Specific Gene Which Is Adjacent to the *Drosophila* Myosin Heavy-Chain Gene and Can Encode a Cytochrome *b* Related Protein. *Nucleic Acids Research* **17**, 6349–6367 (1989). https://doi.org/10.1093/nar/17.15.6349.

30. Hong, H. P., Datla, N., MacKenzie, S. L. & Qiu, X. Isolation and characterization of a Δ5 FA desaturase from *Pythium irregulare* by heterologous expression in *Saccharomyces cerevisiae* and oilseed crops. *Lipids* **37**, 863–868 (2002).
https://doi.org/10.1007/s11745-002-0972-5.

31. Cho, H. P., Nakamura, M. & Clarke, S. D. Cloning, expression, and fatty acid regulation of the human Δ-5 desaturase. *J. Biol. Chem.* **274**, 37335–37339 (1999). https://doi.org/10.1074/jbc.274.52.37335.

32. Ge, L., Gordon, J. S., Hsuan, C., Stenn, K. & Prouty, S. M. Identification of the Δ-6 desaturase of human sebaceous glands: expression and enzyme activity. *J. Invest. Dermatol.* **120**, 707–714 (2003). https://doi.org/10.1046/j.1523-1747.2003.12123.x.

33. Wang, H. *et al.* Crystal structure of human stearoyl-coenzyme A desaturase in complex with substrate. *Nat. Struct. Mol. Biol.* **22**, 581–585 (2015). https://doi.org/10.1038/nsmb.3049.

34. Takakuwa, N., Kinoshita, M., Oda, Y. & Ohnishi, M. Isolation and Characterization of the Genes Encoding Δ^8-Sphingolipid Desaturase from *Saccharomyces kluyveri* and *Kluyveromyces lactis*. *Curr. Microbiol.* **45**, 459–461 (2002).
https://doi.org/10.1007/s00284-002-3860-0.

35. Cahoon, E. B. *et al.* Production of fatty acid components of meadowfoam oil in somatic soybean embryos. *Plant. Physiol.* **124**, 243-251 (2000). https://doi.org/10.1104/pp.124.1.243.

36. Buček, A. *et al.* Evolution of moth sex pheromone composition by a single amino acid substitution in a fatty acid desaturase. *Proc. Natl. Acad. Sci. USA* **112**, 12586–12591 (2015). https://doi.org/10.1073/pnas.1514566112.

37. Kajikawa, M. *et al.* Production of arachidonic and eicosapentaenoic acids in plants using bryophyte fatty acid Δ6-Desaturase, Δ6-Elongase, and Δ5-Desaturase genes. *Biosci. Biotech. Bioch.* **72**, 435–444 (2008). https://doi.org/10.1271/bbb.70549.

38. Duminil, P., Herrfurth, C., Haslam, T. M. & Feussner, I. Setaphyte VERY-LONG-CHAIN FATTY ACYL DESATURASES impact glycerolipid and sphingolipid metabolism. *J. Exp. Bot.*, erag026 (2026). https://doi.org/10.1093/jxb/erag026.

39. Knutzon, D. S. *et al.* Identification of Δ5-Desaturase from *Mortierella alpina* by Heterologous Expression in Bakers' Yeast and Canola. *J. Biol. Chem.* **273**, 29360–29366 (1998). https://doi.org/10.1074/jbc.273.45.29360.

40. Miyazaki, M., Bruggink, S. M. & Ntambi, J. M. Identification of mouse palmitoyl-coenzyme A Δ9-desaturase. *J. Lipid Res.* **47**, 700–704 (2006). https://doi.org/10.1194/jlr.C500025-JLR200.

41. Semmelmann, F. *et al.* Functional characterisation of two Δ12-desaturases demonstrates targeted production of linoleic acid as pheromone precursor in *Nasonia*. *J. Exp. Biol.* **222**, jeb.201038 (2019). https://doi.org/10.1242/jeb.201038.

42. Monroig, O., Navarro, J. C., Dick, J. R., Alemany, F. & Tocher, D. R. Identification of a Δ5-like fatty acyl desaturase from the cephalopod *Octopus vulgaris* (Cuvier 1797) involved in the biosynthesis of essential fatty acids. *Mar. Biotechnol.* **14**, 411–422 (2012). https://doi.org/10.1007/s10126-011-9423-2.

43. Roelofs, W. L. *et al.* Evolution of moth sex pheromones via ancestral genes. *Proc. Natl. Acad. Sci. USA* **99**, 13621–13626 (2002). https://doi.org/10.1073/pnas.152445399.

44. Park, W. J. *et al.* A novel FADS1 isoform potentiates FADS2-mediated production of eicosanoid precursor fatty acids. *J. Lipid Res.* **53**, 1502–1512 (2012). https://doi.org/10.1194/jlr.M025312.

45. Park, W. J., Kothapalli, K. S. D., Lawrence, P., Tyburczy, C. & Brenna, J. T. An alternate pathway to long-chain polyunsaturates: the FADS2 gene product Δ8-desaturates 20:2*n*–6 and 20:3*n*–3. *J. Lipid Res.* **50**, 1195–1202 (2009). https://doi.org/10.1194/jlr.M800630-JLR200.

46. Kabeya, N. *et al.* Biosynthesis of Polyunsaturated Fatty Acids in Sea Urchins: Molecular and Functional Characterisation of Three Fatty Acyl Desaturases from *Paracentrotus lividus* (Lamark 1816). *PLOS One* **12**, e0169374 (2017). https://doi.org/10.1371/journal.pone.0169374.

47. Domergue, F., Lerchl, J., Zähringer, U. & Heinz, E. Cloning and functional characterization of *Phaeodactylum tricornutum* front-end desaturases involved in eicosapentaenoic acid biosynthesis. *Eur. J. Biochem.* **269**, 4105–4113 (2002). https://doi.org/10.1046/j.1432-1033.2002.03104.x.

48. Kaewsuwan, S. *et al.* Identification and Functional Characterization of the Moss *Physcomitrella patens* Δ^5-Desaturase Gene Involved in Arachidonic and Eicosapentaenoic Acid Biosynthesis. *J. Biol. Chem.* **281**, 21988–21997 (2006). https://doi.org/10.1074/jbc.M603022200.

49. Hornung, E. *et al.* Specific formation of arachidonic acid and eicosapentaenoic acid by a front-end Delta5-desaturase from *Phytophthora megasperma*. *Biochim. Biophys. Acta Mol. Cell Biol. Lipids* **1686**, 181–189 (2005). https://doi.org/10.1016/j.bbalip.2004.11.001.

50. Hao, G., Liu, W., O'Connor, M. & Roelofs, W. L. Acyl-CoA Z9- and Z10-desaturase genes from a New Zealand leafroller moth species, *Planotortrix octo*. *Insect Biochem. Mol. Biol.* **32**, 961–966 (2002). https://doi.org/10.1016/S0965-1748(01)00176-X.

51. Zolfaghari, R., Cifelli, C. J., Banta, M. D. & Ross, A. C. Fatty acid Δ^5-desaturase mRNA is regulated by dietary vitamin A and exogenous retinoic acid in liver of adult rats. *Arch. Biochem. Biophys.* **391**, 8–15 (2001). https://doi.org/10.1006/abbi.2001.2361.

52. Aki, T. *et al.* Molecular Cloning and Functional Characterization of Rat Δ-6 Fatty Acid Desaturase. *Biochem. Bioph. Res. Commun.* **255**, 575–579 (1999). https://doi.org/10.1006/bbrc.1999.0235.

53. Rioux, V. *et al.* Trans-vaccenate is Δ13-desaturated by FADS3 in rodents. *J. Lipid Res.* **54**, 3438–3452 (2013). https://doi.org/10.1194/jlr.M042572.

54. Zhou, X. R. *et al.* Isolation and characterization of genes from the marine microalga *Pavlova salina* encoding three front-end desaturases involved in docosahexaenoic acid biosynthesis. *Phytochemistry* **68**, 785–796 (2007). https://doi.org/10.1016/j.phytochem.2006.12.016.

55. Zhu, G. Y., Koszelak-Rosenblum, M., Connelly, S. M., Dumont, M. E. & Malkowski, M. G. The Crystal Structure of an Integral Membrane Fatty Acid α-Hydroxylase. *J. Biol. Chem.* **290**, 29820–29833 (2015). https://doi.org/10.1074/jbc.M115.680124.

56. Stukey, J. E., Mcdonough, V. M. & Martin, C. E. The *OLE1* Gene of *Saccharomyces cerevisiae* Encodes the Delta-9 Fatty-Acid Desaturase and Can Be Functionally Replaced by the Rat Stearoyl-CoA Desaturase Gene. *J. Biol. Chem.* **265**, 20144–20149 (1990). https://doi.org/10.1016/S0021-9258(17)30481-7.

57. Hastings, N. *et al.* Molecular Cloning and Functional Characterization of Fatty Acyl Desaturase and Elongase cDNAs Involved in the Production of Eicosapentaenoic and Docosahexaenoic Acids from α-Linolenic Acid in Atlantic Salmon (*Salmo salar*). *Mar. Biotechnol.* **6**, 463–474 (2004). https://doi.org/10.1007/s10126-004-3002-8.

58. Castro, L. F. C. *et al.* Functional Desaturase Fads1 (Δ5) and Fads2 (Δ6) Orthologues Evolved before the Origin of Jawed Vertebrates. *PLOS One* **7** (2012). https://doi.org/10.1371/journal.pone.0031950.

59. Monroig, O., Hontoria, F., Varó, I., Tocher, D. R. & Navarro, J. C. Investigating the essential fatty acids in the common cuttlefish *Sepia officinalis* (Mollusca, Cephalopoda): Molecular cloning and functional characterisation of fatty acyl desaturase and elongase. *Aquaculture* **450**, 38–47 (2016). https://doi.org/10.1016/j.aquaculture.2015.07.003.

60. Li, Y. Y. et al. Vertebrate fatty acyl desaturase with Δ4 activity. *Proc. Natl. Acad. Sci. USA* **107**, 16840–16845 (2010). https://doi.org/10.1073/pnas.1008429107.

61. Xia, Y. H., Zhang, Y. N., Ding, B. J., Wang, H. L. & Löfstedt, C. Multi-Functional Desaturases in Two Spodoptera Moths with Δ11 and Δ12 Desaturation Activities. *J. Chem. Ecol.* **45**, 378–387 (2019). https://doi.org/10.1007/s10886-019-01067-3.

62. Rodríguez, S. et al. Expression and evolution of Δ^9 and Δ^{11} desaturase genes in the moth *Spodoptera littoralis*. *Insect Biochem. Mol. Biol.* **34**, 1315–1328 (2004). https://doi.org/10.1016/j.ibmb.2004.09.003.

63. Qiu, X., Hong, H. P. & MacKenzie, S. L. Identification of a Δ4 fatty acid desaturase from *Thraustochytrium* sp. involved in the biosynthesis of docosahexanoic acid by heterologous expression in *Saccharomyces cerevisiae* and *Brassica juncea*. *J. Biol. Chem.* **276**, 31561–31566 (2001). https://doi.org/10.1074/jbc.M102971200.

64. Kabeya, N. et al. A complete enzymatic capacity for biosynthesis of docosahexaenoic acid (DHA, 22:6n–3) exists in the marine Harpacticoida copepod *Tigriopus californicus*. *Open Biol.* **11**, 200402 (2021). https://doi.org/10.1098/rsob.200402.

65. Lou, H. Q. et al. The *Torreya grandis* genome illuminates the origin and evolution of gymnosperm-specific sciadonic acid biosynthesis. *Nat. Commun.* **14** (2023). https://doi.org/10.1038/s41467-023-37038-2.

66. Knipple, D. C. et al. Cloning and functional expression of a cDNA encoding a pheromone gland-specific acyl-CoA Δ^{11}-desaturase of the cabbage looper moth, *Trichoplusia ni*. *Proc. Natl. Acad. Sci. USA* **95**, 15287-15292 (1998). https://doi.org/10.1073/pnas.95.26.15287.